METAL - Multiple Emitters Tracking And Localization system

George Vardakis

Thesis submitted in partial fulfillment of the requirements for the

Masters' of Science degree in Computer Science

University of Crete
School of Sciences and Engineering
Computer Science Department
Voutes University Campus, Heraklion, GR-70013, Crete, Greece

Thesis Advisors: Prof. *Xenofontas Dimitropoulos*
Co-advisor: Dr. *Stefanos Papadakis*

University of Crete
Computer Science Department

METAL - Multiple Emitters Tracking And Localization system

Thesis submitted by
George Vardakis
in partial fulfillment of the requirements for the
Masters' of Science degree in Computer Science

THESIS APPROVAL

Author: ________________________
George Vardakis

Committee approvals: ________________________
Xenofontas Dimitropoulos
Assistant Professor, Thesis Supervisor

____
Athanasios Mouchtaris
Associate Professor, Committee Member

____
Apostolos Traganitis
Emeritus Professor, Committee Member

____
Stefanos Papadakis
Researcher - Visiting Professor, Committee Member

Departmental approval: ________________________
Antonis Argyros
Professor, Director of Graduate Studies

Heraklion, 7/11/2017

Abstract

The concept of localization refers to the estimation of a target's position. Applications can range from geolocational services, to the tracking of patients' whereabouts inside a hospital. The spreading of devices utilizing at least some form of radio frequency communication, has opened the door to even more flexible and robust localization systems. This is due to the fact that their signals, traversing the air, can be used to infer the transmitter's position.

In this work we present Multiple Emitters Tracking And Localization (METAL), a localization system for estimating users' positions in indoor environments which can potentially be used alongside existing infrastracture for telecommunication protocols like IEEE 802.11. METAL utilizes mechanisms and technologies employed widely, in order to perform target position estimation efficiently, such as Multiple Input Multiple Output (MIMO). Systems employing this technique utilize multiple antennas for transmission and reception instead of one, with the purpose to increase the capacity of the communication channel or to improve reception. METAL expolits the MIMO technology in order to infer the position of a transmitter using an antenna array with multiple elements.

For proof of concept we employ our system utilizing Software Defined Radios (SDRs). By the term SDR we refer to systems on which components which were traditionally implemented in hardware,— such as filters, modulators/demodulators— are instead implemented in software. The flexibility of such systems is enormous since they can easily adapt to almost any communication protocol and any radio frequency. This trait has brought great popularity to the SDR domain over the past years and has enabled systems like METAL to be much easier implemented and tested.

In our work we explore the benefits and drawbacks of combining SDR and MIMO technologies for localization purposes. In our quest for creating an antenna array using multiple SDR devices, we succesfully combat the essential problem of time-synchronizing the receiving streams of the SDR devices of our system. This is done by employing an over-the-air, low-cost technique using the long training sequence of the IEEE 802.11 protocol, which is capable of synchronizing a large number devices at the same time. Furthermore we examine the type of array that presents the best performance in localization scenarios by comparing some of the most widely used array geometries. Finally, our localization algorithm ,along with the mechanisms for dealing with multiple reflected signals, is presented. We demonstrate that our system is superior to similar ones, based on the fact that it can be used with a large number of telecommunication protocols, without being restricted to a single one.

Περίληψη

Το πρόβλημα του εντοπισμού θέσης ανάγεται στην εύρεση των συντεταγμένων ενός κινητού στόχου σε έναν προκαθορισμένο χώρο. Οι εφαρμογές που αξιοποιούν τέτοιου είδους πληροφορία μπορούν να ποικίλουν, από δορυφορικά συστήματα πλοήγησης μέχρι συστήματα παρακολούθησης ασθενών σε νοσοκομεία και άλλους εσωτερικούς χώρους. Η εξάπλωση συσκευών που αξιοποιούν τουλάχιστον κάποια μορφή ασύρματης επικοινωνίας έχει ανοίξει το δρόμο προς όλο και περισσότερο ευέλικτα και αποδοτικά συστήματα εύρεσης θέσης. Αυτό οφείλεται στο γεγονός οτι τα σήματα αυτών των συσκευών, τα οποία διαδίδονται ελεύθερα στον αέρα, μπορούν να χρησιμοποιηθούν ώστε να εξαχθεί από αυτά η πληροφορία της θέσης του αποστολέα.

Σε αυτή την εργασία παρουσιάζουμε το Multiple Emitter Tracking and Localization (METAL), ένα σύστημα εντοπισμού θέσης για εσωτερικούς χώρους. Το METAL μπορεί δυνητικά να εφαρμοστεί πάνω από ήδη υπάρχουσες υποδομες για τηλεπικοινωνιακά πρωτόκολλα. Χρησιμοποιεί μηχανισμούς και τεχνικές που είναι ευρέως εφαρμοσμένες σε τηλεπικοινωνιακά συστήματα, με σκοπό την εύρεση θέσης ενός στόχου με όσο το δυνατόν πιο αποτελεσματικό τρόπο. Μια τέτοια τεχνική αποτελεί η Πολλαπλή Είσοδος Πολλαπλή Έξοδος (Multiple Input Multiple Output - MIMO). Τα συστήματα που χρησιμοποιούν τη συγκεκριμένη τεχνική επιστρατεύουν τη χρήση πολλαπλών κεραιών για λήψη και μετάδοση αντί για μία, με στόχο την αύξηση της χωρητικότητας του καναλιού ή τη βελτίωση του ληφθέντος σήματος. Το METAL εκμεταλλεύεται την τεχνολογία MIMO με σκοπό την εύρεση θέσης πολλαπλών πομπών, χρησιμοποιώντας μία συστοιχία κεραιών, πολλαπλές δηλαδή κεραίες οργανωμένες σε μία δομή.

Για το πρωτότυπο σύστημά μας χρησιμοποιήσαμε πομποδέκτες διαμορφούμενους από λογισμικό (Software Defined Radios - SDRs). Με τον όρο αυτόν αναφερόμαστε σε συστήματα των οποίων τα επιμέρους κυκλώματα τα οποία παραδοσιακά ήταν υλοποιημένα σε υλικό (hardware) πλέον υλοποιούνται σε λογισμικό (software). Η ευελιξία τέτοιων συστημάτων είναι τεράστια, καθώς μπορούν να προσαρμοστούν σε ένα πολύ μεγάλο εύρος τηκλεπικοινωνιακών συχνοτήτων και να υλοποιήσουν οποιοδήποτε πρωτόκολλο επικοινωνίας. Αυτά τα πλεονεκτήματα έχουν φέρει μεγάλη δημοτικότητα στα SDRs τα τελευταία χρόνια, δίνοντας τη δυνατότητα σε συστήματα όπως το METAL να υλοποιηθούν και να εξεταστούν.

Σε αυτή τη δουλειά ερευνάμε τα πλεονεκτήματα και μειονεκτήματα της συνεργατικής χρήσης SDR και MIMO τεχνολογιών με σκοπό την εύρεση θέσης στόχων. Στην προσπάθειά μας να δημιουργήσουμε την κατάλληλη συστοιχία κεραιών για τις ανάγκες μας χρησιμοποιώντας πολλαπλές συσκευές SDR, καταφέρνουμε να επιλύσουμε το σημαντικό ζήτημα του συγχρονισμού των συσκευών του συστήματός μας. Αυτό το επιτυγχάνουμε εφαρμόζοντας μία ασύρματη, χαμηλού κόστους τεχνική που αξιοποιεί την ειδική σηματοσειρά long

training sequence του πρωτοκόλλου IEEE 802.11, κάτι που μας επιτρέπει να συγχρονίσουμε έναν μεγάλο αριθμό συσκευών ταυτόχρονα. Επιπλέον, εξετάζουμε ποιά δομή για τη συστοιχία κεραιών μας παρουσιάζει τις καλύτερες επιδόσεις σε εφαρμογές εύρεσης θέσης, συγκρίνοντας μερικές από τις πιο διαδεδομένες στη βιβλιογραφία δομές. Τέλος, ο αλγόριθμος εύρεσης θέσης παράλληλα με τους μηχανισμούς αντιμετώπισης των αποτελεσμάτων που έχει στο λαμβανόμενο σήμα η παρουσία πολλαπλών ανακλασμένων αντιγράφων του αρχικού σήματος, παρουσιάζονται. Δείχνουμε οτι το σύστημά μας υπερτερεί έναντι παρόμοιων λόγω του γεγονότος οτι μπορεί να εφαρμοστεί με ένα μεγάλο εύρος τηλεπικοινωνιακών πρωτοκόλλων, χωρίς να περιορίζεται μόνο σε ένα.

Acknowledgements

I would like to thank my supervisors, Mr. Xenofontas Dimitropoulos and Stefanos Papadakis for their guidance and help during this work. Special thanks to Manolis Surligas for the crucial help in completing this thesis.

Last, I would like to thank all those people that supported me all over these years.

Contents

List of Figures

List of Tables

Chapter 1

Introduction

1.1 Motivation

Target localization is a field of applications whose origins can be traced back to the 19^{th} century. The introduction of systems performing target position estimation flourished during the early years of the 20^{th} century, mainly for military purposes. In the modern world where the number of devices utilizing at least some form of wireless technology exceeds the number of the population of people, position estimation has found new grounds for expansion. Knowledge of the position of a wireless user can improve significantly their received signal quality by using appropriate techniques at the transmitter. Also the user experience in places such as museums can significantly be enhanced by adapting the projected content according to the position of the visitor. For the extended and most efficient use of such systems both the low-cost criterion and the adaptability of the devices implementing them must be ensured.

Technologies employed for position estimation of a wireless transmitter include Bluetooth beacons, RFIDs, RSSI measurements and fingerprinting. Each of these presents drawbacks, as is for example the low noise resilience of RSSI and fingerprinting, or the sparse presence of Bluetooth nodes in indoor environments. One technology that has been extensively applied in the last years is Direction of Arrival (DoA). This is also not a new concept, since RDFs (Radio Direction Finders) have been used for many decades to infer the direction of arrival of a transmitted signal, but today's extensive deployment of DoA for position estimation purposes has been fueled by the widespread use of Multiple Input Multiple Output (MIMO) technology. MIMO employs multiple antenna elements at the transmitter and receiver with the goal of either increasing the channel capacity or mitigating the effects of the channel on the transmitted signal. Multiple antennas can also be used for DoA estimation. This reality has driven more and more applications towards combining MIMO and DoA techniques for position estimation, since this field can benefit from the attractive characteristics of DoA such as resilience to noise and low computational complexity.

The next consideration regards what type of signals and protocols can be used to identify and localize users. For indoor localization - which will be the focus of this study - a main concern is to use as less extra infrastructure as possible. The ideal scenario includes the implementation of localization functionality using the existing infrastructure so that the overall cost remains low and the complexity of installment of a localization system is as low as possible. Protocols used in indoor communications include the IEEE 802.11 protocol

(WiFI) or the IEEE 802.15.4 protocol for sensor networks. The utilization of such protocols for a low-cost, flexible localization application offers a variety of advantages. First they are present in most indoor places and supported by most mobile devices. Second, no intervention to the existing infrastracture is required since the various base stations can be used for localizing targets. Adding to that, using the system along with such a protocol allows the exploitation of mechanisms present in the standards, to solve problems inherent to the DoA estimation and localization. One major problem is the multipath fading, while another one is the mapping of signals detected to the users or devices that these signals originated from. Both these problems can be addressed with the exploitation of many of the protocols' mechanisms and functions.

1.2 Related Work

For the DoA estimation problem various algorithms have been studied over the years. MUSIC [1] and Estimation Of Signal Parameters via Rotational Invariance Techinques (ESPRIT) [2] are two of the most prominent algorithms in the literature related to direction finding of electromagnetic signals. They both employ subspace manipulation, namely they decompose the observation space into the signal and the noise subspace which subsequently they exploit to find the angles of arrival. Minimum Variance Distortionless Response (MVDR) is the most popular conventional method for DoA. It uses beamforming and properly adjusted array weights to detect the direction of arrival of signals.

Many works have concentrated on overcoming inherent limitations presented by algorithms such as MUSIC or ESPRIT. These limitations include the eigenvalue decomposition that is required which is generally a computationally expensive process or the assumption that signals come from the far field resulting in a plane wave arriving at the array. The works in [3, 4] deal with the near-field sources scenario, while the work in [5] uses the propagator method in [6] to avoid the singular value decomposition. The problem of estimating the range and frequency of signal sources is considered in [4], while the detection and parameter estimation of wideband sources is considered in [7, 8].

A great number of publications has dealt with the implementation of these algorithms in the context of direction finding both in azimuth and in elevation, with the type of the array configuration always playing a crucial role to the efficiency of the system. The array setups that have been studied include Rectangular arrays [9], Circular arrays [10, 11, 9], and L-shaped arrays [12, 13, 14]. Some even more complex configurations have been considered such as the split vertical linear and Circular array [15], the triangular pyramid array for sound DoA estimation [16], or the cylindrical array [17].

A lot works have focused on the issue of localization using WiFi. The approach of CUPID [18] is to estimate the position of a user, by exploiting the Channel State Information of the packets sent by that user as well as the mobility of them. Although it achieves a median error of 2.7 meters just with one AP, CUPID requires that an application runs on the user's device and uses sensors like the gyroscope in order to infer the distance the user has covered and hence deduct the Angle of Arrival of their signal using MUSIC. This can prove to be energy consuming and is not easily applicable since the user must install an extra application. PinLoc [19] also uses PHY information to infer position. It uses the Channel Frequency Response of each OFDM subcarrier to form fingerprints for every location in space and then match the fingerprints of each user to the pre-calculated ones of the observed space. That requires an algorithm to compute the fingerprints for each location in space prior to deployment of the system. SpotFi [20] utilizes Channel State Information across subcarriers as well as RSSI measurements and calculates both time of flight and angle of arrival of signals to detect the direct path in a multipath environment and consequently infer position. The drawback is that it relies on WiFi for its function. Furthermore, RSSI measurements are prone to fluctuations due to varying noise conditions.

1.3 Contribution

In this work we present Multiple Emitters Tracking And Localization (METAL), a localization system which utilizes MIMO technology along with a communications protocol. The system is presented and evaluated using various metrics. Next we examine the role that the geometry of the antenna array plays in the estimation process and we present an extensive comparison of some of the most popular array configurations in the area of DoA. To our knowledge this is the first evaluation of its kind. Finally we present our real-time DoA prototype system for which we employed the use of Software Defined Radio (SDR) devices i.e. flexible RF transponders. The utilization of SDR hardware for implementing localization systems is an attractive option both for the flexibility in the choice of many parameters of the system such as the frequency used, the protocols supported or even the antenna array that will be used as well as for the testing capabilities they provide. However suitable they may be though, they also suffer from various hardware-related problems or wireless transmission phenomena. In this context we time-synchronize the different SDR devices using the long training sequence of IEEE 802.11 protocol, a newly applied technique for synchronizing SDR devices in a low-cost fashion.

Chapter 2

Background

2.1 MIMO

2.1.1 History

MIMO is an RF technique utilizing multiple antennas at the transmitter and the receiver. This redundancy in the number of antennas offers the possibility of space-time processing: Multiple Antennas in different positions can be used either to provide increased channel capacity, or increased signal-to-noise ratio by combining both time and space dimensions [21].

The idea of using excessive number of antennas at the endpoints of a communications system is not new. The so-called smart antennas were employed for many years with the goal of direction finding or increasing the gain at certain directions. These early systems were only able to transmit the same stream from all antennas, only changing the phase and gain of the signal of each element. On the receive side the outputs of the antennas were combined accordingly to improve the perceived signal-to-noise ratio. Another option was to use only a subset of the antennas, the ones with the less impaired received signal, again with the goal of improving the overall reception.

As the levels of processing power available started to rise, even more complex realizations of space-time processing became possible. Instead of just mitigating the effects of multipath fading, the newer systems took advantage of the various paths the signal from the transmitter took, creating what was effectively additional channels capable of carrying useful information.

2.1.2 Diversity modes

In the traditional sense of the term, diversity refers to the heterogeneity of the members of a group. In communications diversity is used to make the systems more robust and resilient even to varying channel conditions. This is done by providing the receiver with multiple copies of the signal. If each copy is affected differently by the channel conditions then the probability that all signals will be affected negatively at the same time is considerably small. For this reason diversity improves the error rate and stabilizes the link. The most common forms of diversity are:

- *Time diversity*: With time diversity, a message may be transmitted at different time slots and in conjunction with channel coding.

- *Frequency diversity*: With this scheme a large number of frequencies or channels are utilized for transmission. Such is the case in systems as Spread Spectrum or OFDM.
- *Space diversity*: Space diversity uses antenna elements placed at different locations. The notion behind this technique is that even the smallest displacement of an antenna can change the observed signal since a different set of paths will be combined at the new location.

Space diversity is the basis of MIMO. In essence, multiple antennas are used to provide the receiver with an increased number of signal paths. This was previously regarded as a destructive phenomenon for wireless telecommunications. MIMO systems use this at their advantage to increase the link capacity or reduce the error rate.

There are three formats for MIMO :

- *Spatial Diversity* : Spatial Diversity is a mode of operation used to make the channel more robust and reduce the error rate. It is characterized either by TX or RX diversity, depending on which side of the transmission the excess number of antennas is. RX diversity combines accordingly the multiple copies of the signal coming from the different antennas to increase the signal-to-noise ratio. TX diversity on the other hand transmits redundantly the same signal from all elements, by encoding the desired signal using Space-Time Codes. This method significantly reduces Bit Error Rate in signal transmissions. Alamouti [22] developed the first Space-Time Codes for such systems.
- *Spatial Multiplexing* : Using Spatial Multiplexing the increase of the data rate of the channel is possible, while still obeying the Shannon–Hartley theorem [23]. In this scenario the transmitter sends different streams from each antenna. It is possible to increase linearly the capacity of the given channel with every pair of antennas that is added on the system.
- *Beamforming* : The oldest mode of operation for MIMO antenna arrays is Beamforming. It was very early realized that a mechanism to increase the gain of a transmitter at a certain direction was required. The rationale behind this was both to improve the received signal-to-noise ratio and to reduce interference at nearby nodes. This idea became feasible with antenna arrays and Beamforming. This technique made it possible to form beam patterns towards desired targets by manipulating the phase and gain of the signals transmitted by each element

A typical MIMO communications channel is shown in Figure 2.1. The signal of each transmitting antenna is received by all receiver antennas providing the base for the Spatial Multiplexing functionality of MIMO systems. The channel is described by the Channel matrix H which contains the channel coefficients h_{00} ,h_{01}, h_{10}, h_{11} which in turn describe the individual channel between each pair of receiving and transmitting antenna.

2.1.3 Phased Antenna Arrays

MIMO make use of special structures called Phased Antenna Arrays. In antenna theory a phased array refers to an array of antennas capable of electronically steering the receiving or transmitting beam towards desired directions by introducing phase offsets between the different streams. This means that the energy of the superimposed signals can be maximized at a target in a given direction when transmitting, and the signal from a desired target in a certain direction can be enhanced to achieve better signal-to-noise ratio

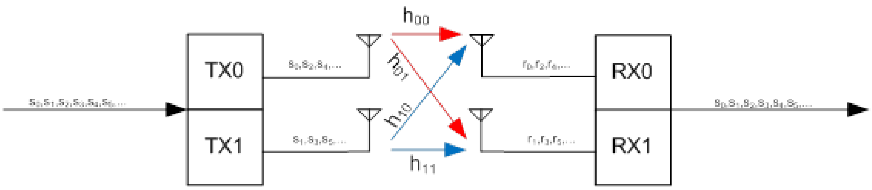

Figure 2.1: MIMO channel

when receiving. By choosing proper weights with which each output is scaled as well as the proper geometry for the array, it is possible to cancel out interference from undesirable directions and receive more sensitively from others.

An important part of the design process of an antenna array is the selection of the number of antennas as well as the distance between them. In general the performance of an array increases as more antennas are used, but with the overall size, complexity and ultimately the cost increasing as well. The spacing of the antennas can either be uniform or non-uniform. In the first case the spacing remains the same between the successive elements, while in the non-uniform case the spacing may alternate between elements. For the selection of the proper spacing, the frequency of the signals for which the array will be used plays a crucial role. In most cases the spacing is selected according to the wavelength lambda (λ) of the intended signals. The spacing must be less than that wavelength so that grating lobes and mutual coupling of the antennas is avoided. Half-wavelength spacing is the most common choice in the literature.

The geometry of the array also poses a challenge when designing an array for an application. An extended study on various array geometries and their performance will be presented in Section 3. Figure 2.2 shows a planar array lying on the xy plane with M rows and N columns and spacing $\frac{\lambda}{2}$

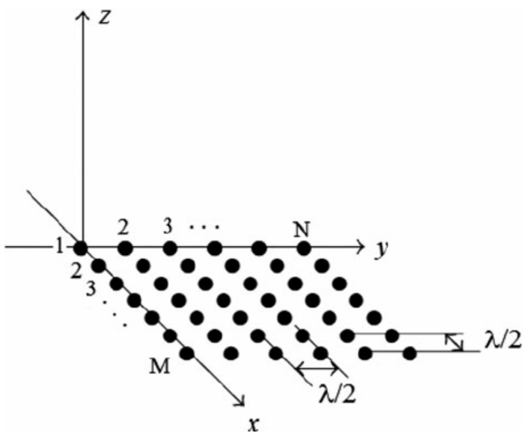

Figure 2.2: Antenna Array

2.1.4 Radars and Direction of Arrival

It did not take long to realize that the flexibility provided by MIMO and phased antenna arrays could offer great potential to a great number of Radio Frequency applications. One such application, that could benefit by the newly introduced MIMO, was radars. Until the 90's traditional radar technologies used an electromagnetic pulse which was transmitted, then reflected on the target's surface and finally arrived back at the transmitter's antenna. Various parameters such as velocity, range or bearing could be estimated by calculating the round trip time of the pulse. To this end a directional antenna was used to transmit the pulse to a specific direction and measure the reflected energy.

The introduction of antenna arrays brought a revolution to the concept of radars. At first, an array could be used for the reception of the reflected pulse. This way, omnidirectional antenna elements could be utilized for transmission of the pulse while the array became responsible for estimating the parameters of the target by taking advantage of the difference in phase of the observed signals from the different antenna elements. The omnidirectional transmitting element was not a very attractive solution though, because of its relatively low gain. An antenna array along with beamforming techniques could be used at the transmitting side, eradicating at the same time the need for moving mechanical parts.

There are two main types of radars:

- **Active Radars** : The most common type of radar is the Active Radar. As mentioned before, a signal is emmited from the transmitting antenna, reflects off target objects and finally returns to the transmitter, who infers target parameters through calculating the time of flight of the pulse.

- **Passive Radars** : In the broader sense, a passive radar does not transmit a pulse in order to identify possible targets. Instead it uses signals from other sources. These sources may be third parties transmitting some kind of signal, which reaches the radar in two copies: One directly and one reflected on the target. The radar can then estimate the desired parameters by measuring the time difference of arrival between the two copies. Additionally, a target can transmit a signal by itself, and a passive radar can utilize that, in order to detect it by utilizing the phase offsets between received antennas' signals.

In this work, passive radars for self-illuminating targets will be examined. The estimation process is carried out by a direction finding algorithm. The most prominent of these include MUSIC, ESPRIT and MVDR. MUSIC will be the algorithm used by our system. The reasoning behind the selection is that MUSIC has been widely used during the last years over the rest of the algorithms, in a variety of applications ranging from the lower frequencies and voice detection, to higher frequencies and WiFi localization. Also it requires considerably less antennas than ESPRIT which makes the real deployment of a system running it less complex. Finally MUSIC achieves higher performance as the number of antennas increases, and as the work in [24] suggests, it has a lower average estimation error.

2.2 MUSIC

Our algorithm of choice for direction finding is MUSIC. To explain the algorithm in depth, the data model of our signals has to be presented first.

We assume that the signal arriving at an arbitrary array is a plane wave. It is mathematically represented as $x(t), t = 1, 2, ..., K$ where K is the number of samples. The output of the array is expressed as

$$X(t) = Ax(t) + n(t) \qquad t = 1, \cdots, K \tag{2.1}$$

where n is zero mean Additive White Gaussian Noise, and A is the steering vector defined as

$$A = \begin{bmatrix} e^{j\frac{2\pi}{\lambda}u_1} & e^{j\frac{2\pi}{\lambda}u_2} & \cdots & e^{j\frac{2\pi}{\lambda}u_N} \end{bmatrix}^T \tag{2.2}$$

where λ is the wavelength of the signal and u_n is the unit vector in direction (ϕ, θ) for sensor n and is defined as

$$\begin{aligned} u_n(\phi, \theta) = d_{x_n} \cos(\theta)\cos(\phi) + d_{y_n} \cos(\theta) sin(\phi) \\ + d_{z_n} \sin(\theta) \end{aligned} \tag{2.3}$$

with $(d_{x_n}, d_{y_n}, d_{z_n})$ being the position vector of the element n

MUSIC is part of a family of algorithms called subspace algorithms. This is because the observation space represented by the received signal at the array is used to find the signal and noise subspaces, which are consequently used to estimate the angles of arrival. To acquire the two subspaces, the spectral matrix S_x has to be computed first, and it is defined as

$$\begin{aligned} S_x &= E\{X(t)X^H(t)\} \\ &= \frac{1}{K}\sum_{t=1}^{K} X(t)X^H(t) \end{aligned} \tag{2.4}$$

with X(t) defined in (1). S_x can be written in terms of its eigenvectors and eigenvalues as

$$S_x = \Phi\Lambda\Phi^H$$

where $\Lambda = diag[\lambda_1, \lambda_2, \cdots, \lambda_N]$, the eigenvalues of S_x and Φ the corresponding eigenvectors.

Assuming that there are D uncorrelated signals impinging on the array, after sorting the eigenvalues and their respective eigenvectors in decreasing order, the noise subspace is defined as

$$U_n = [\Phi_{D+1} \vdots\, \Phi_{D+2} \vdots \cdots \vdots \Phi_N] \tag{2.5}$$

In order to perform direction finding, the following realization must be done. The array steering vector A spans the signal subspace, and the noise & signal subspace are assumed to be perpendicular to each other. If we take the projection of $A(\phi, \theta)$ onto U_n for all desirable values of (ϕ, θ), then the azimuth and elevation pair whose projection is zero, is also the direction of arrival. In terms of mathematical representation, the above is expressed as follows

$$A^H(\phi, \theta)U_nU_n^HA(\phi, \theta) = 0 \tag{2.6}$$

for a signal arriving from (ϕ, θ).

The MUSIC pseudospectrum is then found for all azimuth and elevation pairs, and is expressed as

$$Q_{MUSIC} = \frac{1}{A^H(\phi, \theta)U_nU_n^HA(\phi, \theta)} \tag{2.7}$$

The summarized MUSIC process is presented in Algorithm 1

Data: Signal
`/* Construct the steering vectors */`
for ϕ *in range of* ϕ **do**
  for θ *in range of* θ **do**
    for *Antenna* k **do**
      compute steeringvector[ϕ,θ,k]
    end
  end
end
R ← covariancematrix(signal)
Q ← eigenvectors(R)
I ← eigenvalues(R)
Qs ← eigenvectors corresponding to largest eigenvalues
Qn ← eigenvectors corresponding to smallest eigenvalues
`/* Loop through the observation space and find the MUSIC pseudospectrum */`
for ϕ *in range of* ϕ **do**
  for θ *in range of* θ **do**
    vec ← steeringvector[ϕ,θ]
    Pseudospectrum(ϕ,θ) ← $\frac{1}{vec^H * Qn * Qn^H * vec}$
  end
end

Algorithm 1: MUSIC algorithm

For the implementation of MUSIC on GNU Radio the Armadillo C++ library [25] was used. Armadillo is a high speed, high-level syntax library for the execution of linear algebra calculations like matrix addition, multiplication and eigenvalue decomposition required in the implementation of MUSIC algorithm. One of the main advantages of Armadillo is its speed. Apart from the use of Single Instruction, Multiple Data (SIMD) instructions it also makes use of the openBLAS [26] and LAPACK [27] libraries for more complex operations like eigenvalue decomposition. Also it employs a delayed evaluation approach to combine several operations into one and reduce the need for temporaries making a suitable candidate library for implementing MUSIC in real-time scenarios.

2.3 Frequency and Phase Synchronization

As we've shown MIMO systems offer attractive features to communication applications. For a system to successfully perform DoA estimation the following requirements must be met:

- *Frequency Synchronization* : The signal components in the different receiving channels must have identical frequencies

- *Timing Synchronization* : All Digital Processing operations at the receiving channels must be performed on samples that are aligned in time

2.3.1 Frequency Synchronization

Frequency synchronization refers to the problem of synchronizing the receiving channels of a MIMO system in frequency. Most communication protocols specify a level of tolerance of frequency offset between transceivers and at the same time deploy mechanisms in the receiver side for counteracting the effects of it.In a typical communication system, carrier frequency offset (CFO) causes Inter Symbol Interference (ISI) which leads to reduced SNR. For a MIMO DoA estimator, even a small offset can have devastating effects on the performance.

Two signals with different frequencies have in essence a constantly changing phase offset. As long as the frequencies of the signals remain the same, the rate at which this offset changes is stable. Since direction of arrival techniques leverage the relative phase difference to infer position, this phenomenon causes the estimation to rotate constantly around the observation space, at the rate at which the relative phase changes.

In Figure 2.3 two signals with frequency offset are depicted. Even a few Herz of offset - 100 in this case - can alternate significantly the phase offset between them in a short period of time.

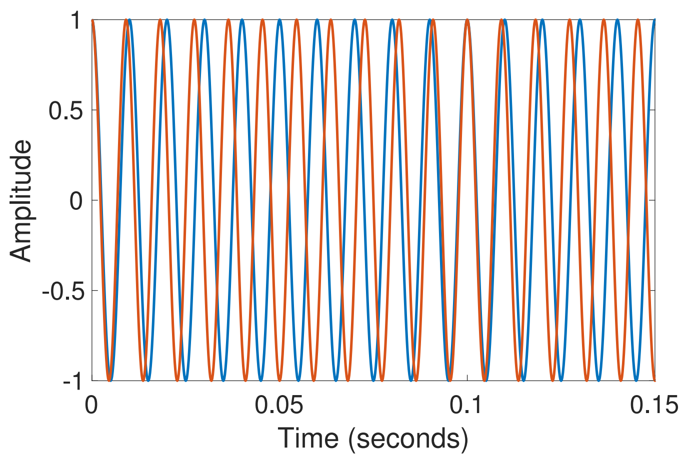

Figure 2.3: Frequency Offset

2.3.2 Timing and Phase Synchronization

Timing is another important aspect of MIMO DoA systems. This means that the samples that are fed to the Digital Processing units must be aligned in time i.e. they must be sampled at the exact same time instance. Absence of time synchronization between receiving channels can introduce arbitrary phase offsets between the different streams and corrupt the existing information about the phase offset induced by position inside the streams. Figure 2.4 indicates this problem. Here the blue curve illustrates the ideal signal received by one stream, sampled at the proper time instants, while the red curve shows the received signal of another stream, which is not sampled at the same points, something which introduces phase offset between them.

Another restriction placed on DoA applications is that a known and constant phase relationship between the input RF streams must be maintained in order to have a reliable direction estimation. This relation can be compromised by various factors such as phased-locked loops that may reside in the system for up and down-conversion or for clock synchronization. Other factors include filters, mixers and amplifiers who can introduce phase noise varying with time, temperature or mechanical conditions.

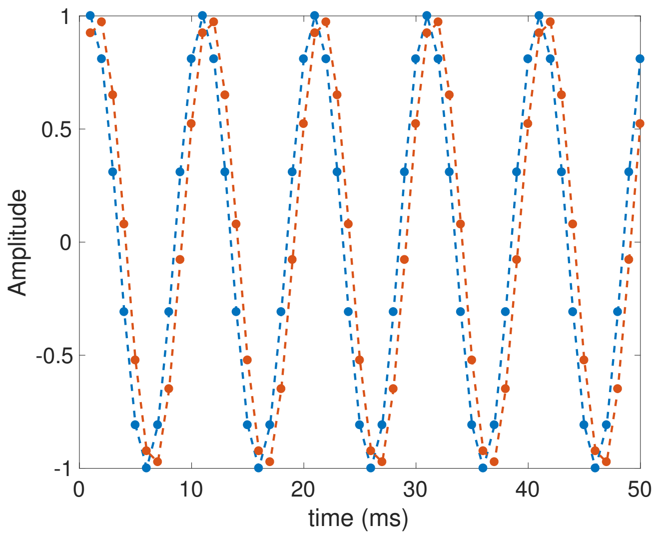

Figure 2.4: Sample Time Offset

2.4 Localization System

The problem of finding the exact position of a user or target does not have a straightforward approach. The two parameters that need to be identified are the angle of arrival of a signal coming from the target, and its range i.e. the distance of the array to it. An active localization system may transmit a signal which after bouncing on the target will return to the array, while a passive one exploits the signals sent by the target, both attempting to infer the two parameters mentioned. In an attempt to make a localization system that is as less invasive as possible, in the sense that no extra infrastructure is needed for the system to work, we focused our attention on creating a passive system, exploiting existing

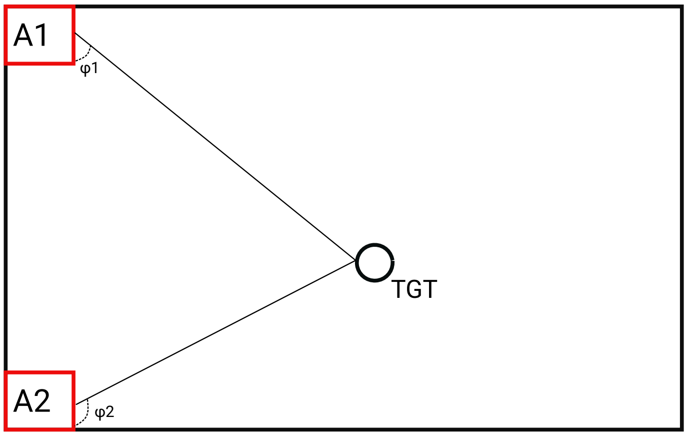

Figure 2.5: METAL system setup

communication protocols and their infrastructure. Our algorithms and simulations will be based on the IEEE 802.11 protocol because of its extended use and applicability in almost every mobile device. The principals and ideas implemented are not limited to the specific protocol. Any protocol that employs similar mechanisms can use METAL for target tracking and localization.

2.4.1 Position Estimation

A target's position can be determined by a single antenna array. This can be achieved by estimating the angle of arrival of the signal as well as its time of flight. The estimation of time can be a very complex procedure and a not accurate one. For this reason our approach utilizes two arrays, with known positions. As Figure 2.5 shows, the DoA estimation algorithm runs on two arrays. Each one determines the angle of arrival of the signal originating from a target (TGT). Then with the proper calculations the intersection of the two lines expanding from each of the arrays towards the determined direction is regarded as the target's position.

For a set of arrays operating in the azimuth plane only, the position of a target can be found by solving the following system of equations:

$$\begin{aligned} y - y_1 &= \phi_1(x - x_1) \\ y - y_2 &= \phi_2(x - x_2) \end{aligned} \tag{2.8}$$

where x_1, y_1 and x_2, y_2 the positions of the arrays and ϕ_1 , ϕ_2 the estimated angles.

If the system is also observing the elevation plane, the above two-dimensional problem is deduced to a three-dimensional one. To solve it given the ϕ_1, θ_1 and ϕ_2, θ_2 estimated by the arrays, we first need to create two lines in space, the intersection of which will be the position of the target. Each of the two lines as in the previous problem will go through one array and will have the direction of the estimated angle. Firstly we find a point on each one of the lines which is preferably out of the space or room we are observing. This point is given by:

$$
\begin{aligned}
x &= r * cos(\theta) * cos(\phi) \\
y &= r * cos(\theta) * sin(\phi) \\
z &= r * sin(\theta)
\end{aligned} \tag{2.9}
$$

where r is the range. We set it to a large value for this estimation so that it falls out of our observation space. Now we have two points for each line. The lines can be described mathematically as :

$$
\begin{aligned}
&BS1 + a * [P_1 - BS1] \\
&BS2 + b * [P_2 - BS2]
\end{aligned} \tag{2.10}
$$

where $BS1$, $BS2$ the cartesian coordinates of the base stations and P_1, P_2 the coordinates of the points on the two lines we found using Equation 2.9. The task now is to find the two points on each line that minimize the distance between them. We will define these points as:

$$
\begin{aligned}
L_1(s) &= BS1 + s * [P_1 - BS1] \\
L_2(r) &= BS2 + r * [P_2 - BS2]
\end{aligned} \tag{2.11}
$$

A vector on the line connecting these two points $(L_2(r) - L_1(s))$ will be perpendicular to the vectors in the directions of the two lines. Let's denote as $V1$ the vector in the direction of the first line and as $V2$ the vector of the second line. Each one of them is defined as:

$$
\begin{aligned}
V1 &= [P_1 - BS1] \\
V2 &= [P_2 - BS2]
\end{aligned} \tag{2.12}
$$

Taking advantage of the perpendicularity we have:

$$
\begin{aligned}
&(L_2(r) - L_1(s)) * V1 = 0 \\
&(L_2(r) - L_1(s)) * V2 = 0
\end{aligned} \tag{2.13}
$$

Solving the above system of two equations with two unknowns yields the s and t values required to identify the points $L_2(r)$ and $L_1(s)$. If the two points are not identical, meaning that the two lines don't intersect, we consider the point in the middle of the line connecting them as the target position.

2.4.2 Multipath Reflections

The phenomenon where multiple delayed copies of a signal caused by reflections in the surrounding environment reach a receiving node along with the original signal, is called multipath. A simple multipath scenario with one direct and two reflected components is shown in Figure 2.6. A DoA estimation algorithm like MUSIC will distinguish the angles of arrival of the multiple superimposed copies of the signal in the observation under certain conditions: First, the multipath components must have enough power to be

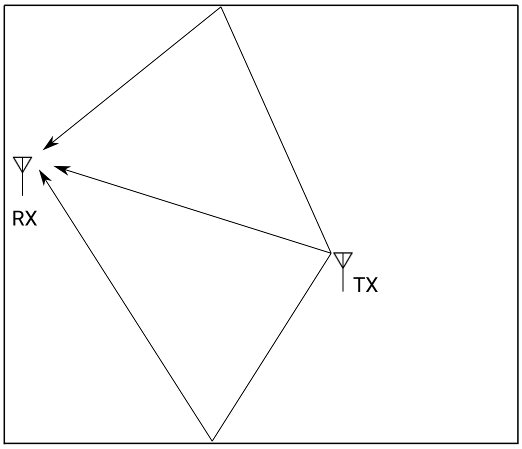

Figure 2.6: Multipath reflections

detected. Second, due to limitations of MUSIC algorithm the number of components in an observation has to be smaller or equal to the number of antennas otherwise the paths will not be distinguished.

An efficient localization system must be able to distinguish betwen the direct path signal and the reflected copies in order to determine the right DoA. This can be achieved either by canceling out the multipath components in the observation, or by determining the angle corresponding to the direct path component. One realization that can be done towards achieving the latter option, is that the direct path component will be the first to arrive at the receiver since it follows the shortest (direct) path. Our system exploits this idea in order to detect the angle corresponding to the direct path.

As was mentioned before, MUSIC is capable of determining the angle of multiple signals existing in a set of samples. Another interesting fact is that signal with the highest power will also have a higher value in the pseudospectrum reported by the algorithm. In most cases the direct signal will also have the highest power compared to the reflected components, so MUSIC detects its angle giving at the same time the greatest value in the pseudospectrum. There are some cases though, where one or more of the reflected components will have higher power because of the surface on which they were reflected. In these cases MUSIC will mistakenly regard the highest value in the pseudospectrum as the angle of the direct path.

Our intuition was to exploit the training sequence used by most communications protocols. Assuming that the system is aware of the protocol whose signals will be used to locate users, we can cross-correlate the known training sequence with the observed signal. This correlation will give us peak values every time the training sequence is present in the signal, hence a peak value for the direct path and every multipath component. Furthermore, the peak value will be greater as the power of a component increases. Now we have a way to identify the relation of the power of the direct path component to the multipath components, and apply that knowledge to the results of the MUSIC algorithm: If the cross-correlation gives us two peaks, the earlier one lower in power, and the algorithm identifies two angles, one with greater value than the other in the pseudospectrum, then we know that the angle corresponding to the lower value is the direct path component.

For our simulations and tests we assumed our system is used in conjunction with the IEEE 802.11 protocol.The sequence we utilize is the long training sequence which exists at the beginning of every 802.11 packet. For a more clear view, the structure of the training sequence of an Orthogonal Frequency Division Multiplexing (OFDM) modulated 802.11 packet is shown in Figure 2.7. It is constructed by ten repetitions of the short training sequence at the beginning, followed by two repetitions of the long training sequence. If only the original signal exists in a set of samples, then the output of the cross-correlation function will be that of Figure 2.8: Two peaks, one for each repetition of the long training sequence. In Figure 2.9 we can see the cross-correlation output of a signal containing both the direct path and a delayed one. Specifically the delayed component arrives two samples later and with 50% more power at the receiver. Through the correlation output we can clearly see the two sample difference of the peaks, as well as the difference in power.

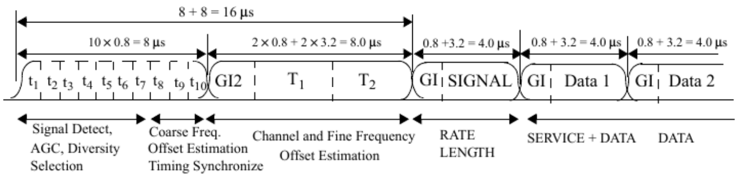

Figure 2.7: OFDM training sequence structure

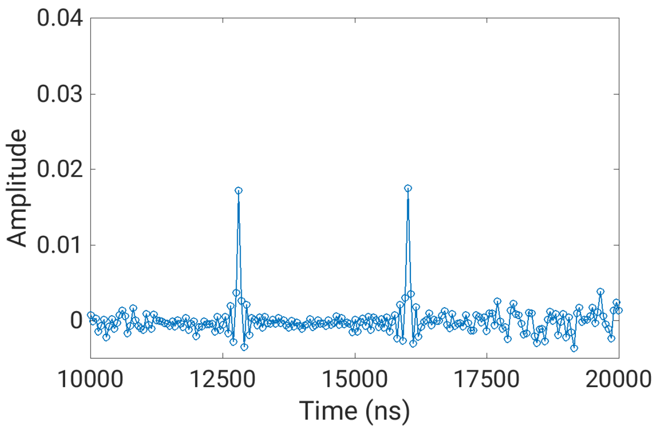

Figure 2.8: Cross-correlation output of one signal component

2.4.3 Target Identification and Outlier Detection

For a big range of applications, just determining the position of a source is not enough. In a crowded indoor environment, where more than one sources coexist, these must also be identified and tagged. To do that, one would need a unique way to indentify each one and distinguish one source from the other. If METAL is used in conjunction with a packet based protocol, we can extract information such as the link layer address of the transmitting device. This is a static address associated with every Network Interface Card (NIC) and can be very conveniently used for mapping a detected position to a specific device or user.

The above information can prove to be very useful for our system. A window of past estimated positions is kept for each user. Depending on the application, we can define a

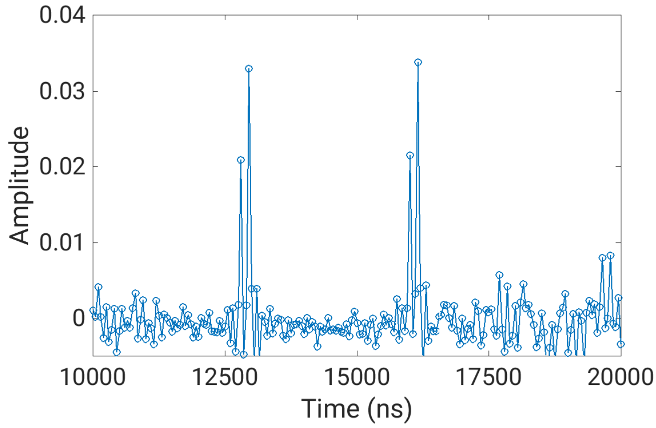

Figure 2.9: Cross-correlation output of a direct and a delayed path

range of expected values for the next estimation, based on past estimations, so that outliers due to failed detection can be eliminated. This elimination takes place in two phases. First, each array identifies abnormal angle estimations. This is done in the following way. Each estimation that is given to the central server, is the result of a number of estimations, each one from every chunk of samples that is provided to MUSIC algorithm. The angles determined by each execution of MUSIC are grouped based on their direction: all angles that fall in the same region are grouped together, while angles that fall far from that region are grouped separately. After each set of estimations, the mean value of the group that holds the most estimated angles are given to the central server. This way, angles that fall far from the prevalent region, are not taken into account. The size of each region can be chosen according to the intended application.

The second phase takes place at the central server. We exploit the information about past positions of a user in order to identify outlying position estimations. To achieve this we define an acceptable radius inside which we expect the estimations to be. This can be also defined according to the application. Estimated positions that fall out of the defined radius are not taken into account, instead the last known position is provided. A more sophisticated outlier detection algorithm could provide even better performance but it is out of the scope of this study.

As mentioned before MUSIC extracts one angle per set of samples examined, the one that corresponds to the direct path component. This implies that if two or more users transmit at the same time and the superimposed signals reach the base stations, only one user will be localized and identified by the system. A way must be found to achieve the presence of the signal of one user per observation set. The advantage of METAL running along a communications protocol, is that most of today's protocols employ mechanisms for medium access control. Such mechanisms make it possible for multiple stations connected to the same medium to share it without their transmissions coinciding. This makes a perfect fit for our requirement, since for every observation window only one station is transmitting. Specifically, the medium access control of IEEE 802.11 shown in Figure 2.10 uses special control frames, namely the Ready to Send (RTS) and Clear to Send (CTS) frames which inform the stations of who is granted access to the medium for transmitting and for how long. This way only one station transmits and the rest defer their transmissions until the medium is free again.

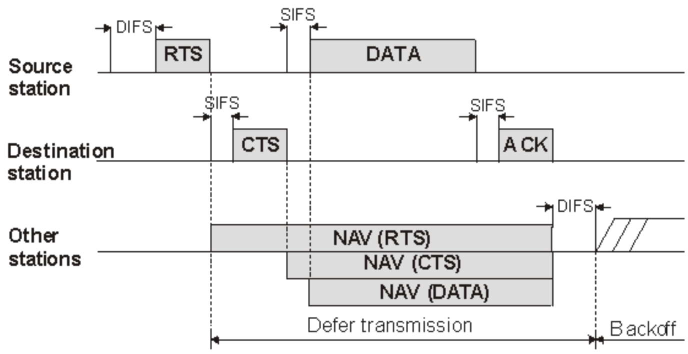

Figure 2.10: Medium Access Control mechanism of IEEE 802.11

Chapter 3

Theoretical Evaluation

3.1 Array Evaluation

In this section the results of our array evaluation will be presented. The notion behind this evaluation is that each configuration exhibits unique characteristics based on its geometry. This makes different arrays suitable for different applications. The question that arises at this point is which of these configurations is the most fitting for our system. For this reason the various array configurations that have been proposed in the literature need to be classified according to their properties. Such properties include the estimation error depending on the direction of the incoming signal, the behavior of the array in cases where the frequency of the incident signal is different than the frequency for which the array was designed, and the ability of the array to distinguish between two or more signal sources.

3.1.1 Array configurations

Some of the most popular array geometries that we will employ in our comparison include the Square, the Circular, and the L-shaped array. We also make a contribution by proposing a new array configuration, which we call Articulated L-shaped array because of its geometry. In essence it is constructed by two square arrays perpendicular to each other, sharing one common edge on the y axis. The hybrid nature of the array - L-shaped using square arrays - allows it to benefit from the characteristics of both configurations. Figure 3.1a shows our prototype configuration which will be used for the simulations.

The inter-element spacing of the elements of all the arrays was selected as one half of the wavelength of the expected signal. In fact, any odd multiple of that quantity is theoretically suitable for direction finding applications. The half wavelength spacing results in the minimization of grating lobes in the beam pattern of the array.

For the Square array we allocated 9 elements in a 3x3 configuration while for the L-shaped array we used 7 elements, 4 on the z and 4 on the x axis, with the element at the origin of the axis common for both linear arrays. The Articulated L-shaped array employs 6 elements, as does the Circular array. The performance of the arrays is analogous to the number of elements deployed, as the simulation results reveal, but we chose to conduct the simulations using a small number of elements for each array so that the cost for a real deployment remains small.

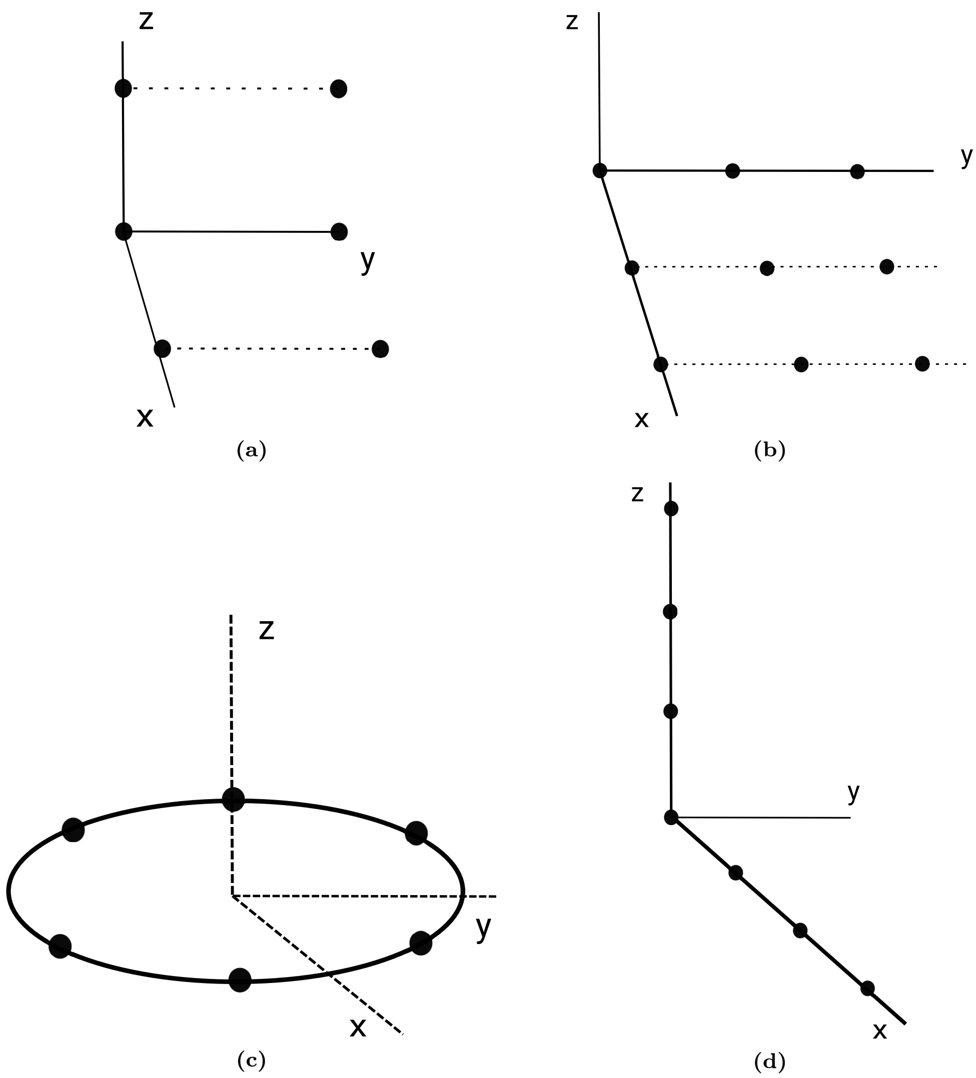

Figure 3.1: Array configurations, (a) Articulated-L-shaped, (b) square, (c) circular and (d) L-shaped

3.1.2 Simulations

The four array configurations were assessed using various metrics. The selection of those metrics was such that a wide variety of characteristics is evaluated.

3.1.2.1 Root Mean Square Error

The first aspect from which we will examine the arrays is that of the error of detection. The Root Mean Square Error is used for this reason and is defined as:

$$RMSE = \sqrt{(\hat{\phi} - \phi)^2 + (\hat{\theta} - \theta)^2}$$

We sampled the observation space at three points : (5,5) (45,45) and (85,85). These specific points were selected because the first and third are at the endfire of the spatial spectrum examined, i.e. at places where the detection is generally difficult, and the second point is the center of that spectrum, offering a higher possibility of detection. We placed the sources at these (azimuth, elevation) pairs and independently for each source calculated the RMSE for different values of the SNR. Figure 3.3 summarizes the results. In Figures 3.2a, 3.2c and 3.2e the RMSE for a narrowband signal source are presented, while Figures 3.2b, 3.2d and 3.2f show the RMSE for a wideband signal. We can see that in the wideband signal case the RMSE is slightly higher because of the higher number of frequencies residing in the signal. The square array has the higher performance in most cases while the articulated L-shaped array performs better in the low azimuth and elevation scenario.

For a more complete view of the performance of the arrays we calculated the RMSE for the positive elevation hemisphere. We placed a signal source at each direction in the interval [0,90] elevation and [-180,180] azimuth with one degree steps. Figure 3.3 presents the results after 1000 independent simulations for each source direction with 0 dB SNR. We tested the Square, the Circular and the Articulated L-shaped array in this fashion. The L-shaped array cannot be evaluated in this way since it cannot differentiate between angles in the negative and positive azimuth.

In Figure 3.3a the hemisphere RMSE for Articulated L-shaped array is shown. The spikes that appear in the regions around integer multiples of π and in low elevations, are due to a mirror signal that appears in those cases and is sometimes stronger than the actual signal.

For the Square array in Figure 3.3b the same spikes as in the Articulated L-shaped array appear. In this case, they are just indicative of the low performance of the Square array in the endfire azimuth regions and at elevation values between 0 and 5 degrees. The Circular array in Figure 3.3c performs significantly well for most directions of arrival.

3.1.2.2 Frequency Mismatch

Next we evaluate the configurations based on their behavior in scenarios when the frequency — hence the wavelength — of the received signal is different from the wavelength used for the calculation of the spacing between the antennas. In typical scenarios the spacing between antenna elements is half a wavelength. Mismatch between the assumed and the real wavelength can deteriorate the DoA estimation.

For the first experiment a source was placed at each direction of the observation space, which we set at 0 - 90 degrees for both azimuth and elevation. The expected frequency of the signal was set to 2.4 GHz and the spacing between the antennas was calculated accordingly. The actual frequency of the signal varied $\pm$ 50 MHz from the expected one.

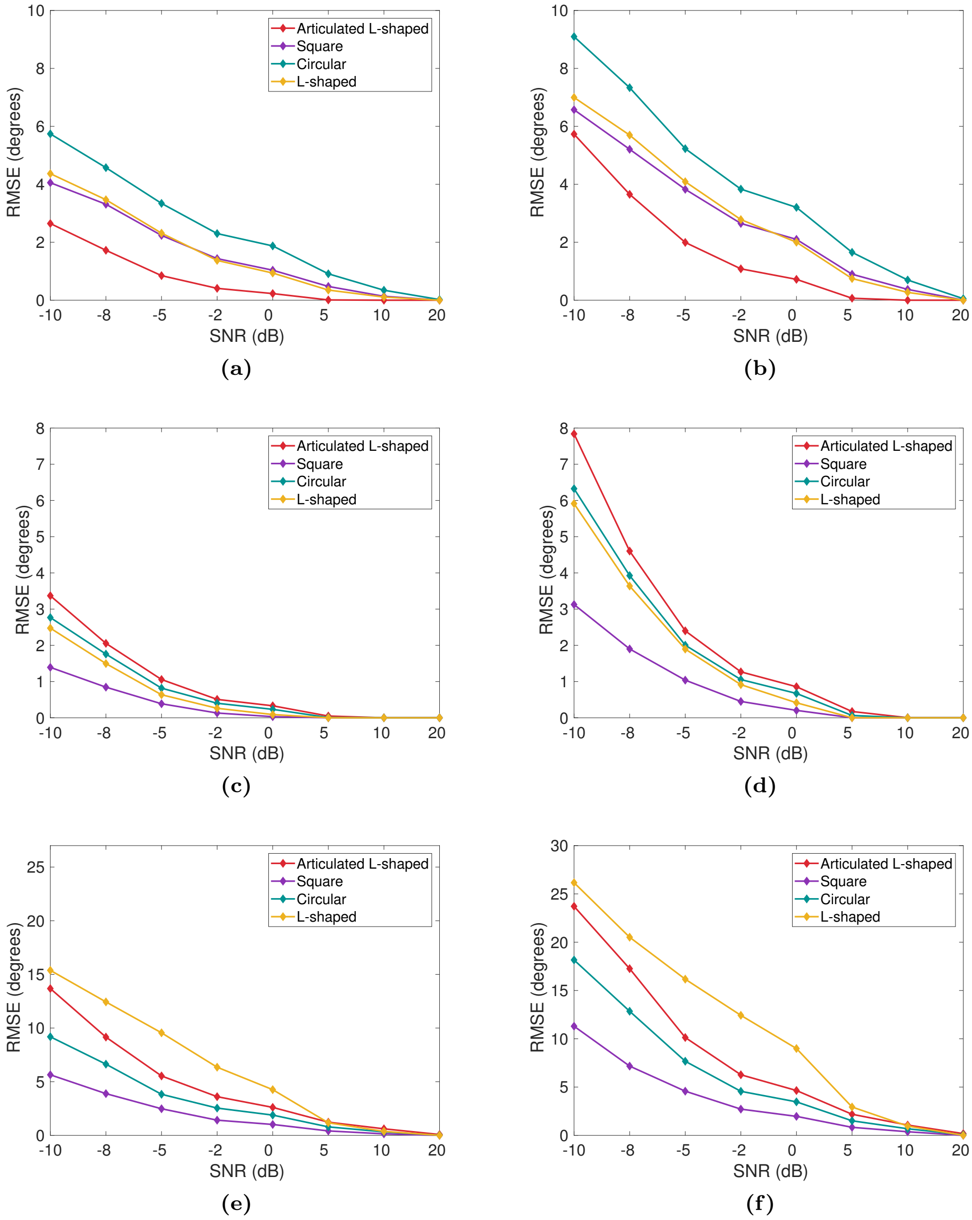

Figure 3.2: RMSE evaluation for (a) (b) ($\phi = 5°$, $\theta = 5°$), (c) (d) ($\phi = 45°$, $\theta = 45°$) and (e) (f) ($\phi = 85°$, $\theta = 85°$) of (a) (c) (e) narrowband and (b) (d) (f) wideband signals

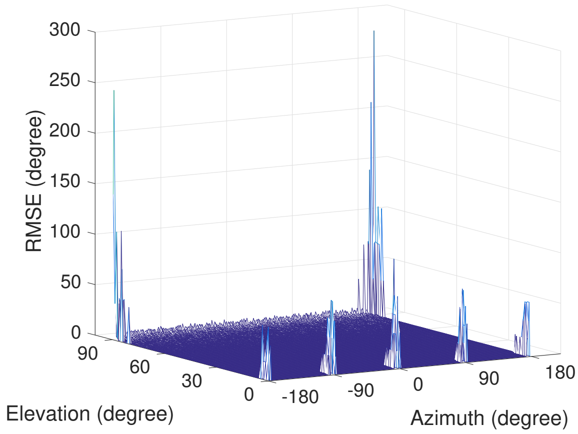

(a)

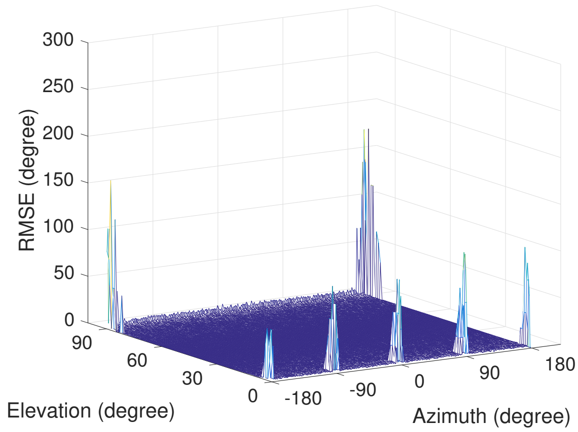

(b)

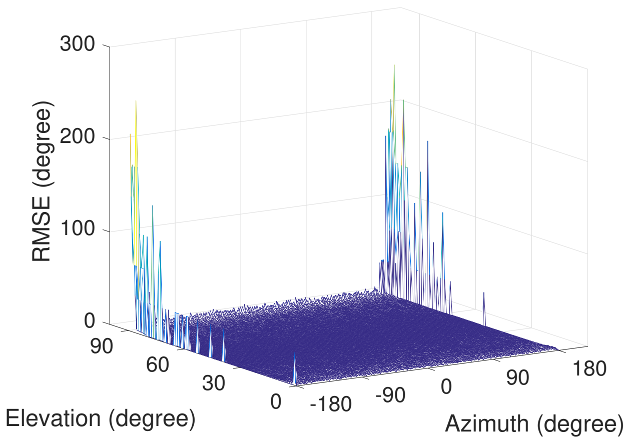

(c)

Figure 3.3: RMSE evaluation of hemisphere for (a) Articulated L-shaped , (b) square and (c) circular arrays

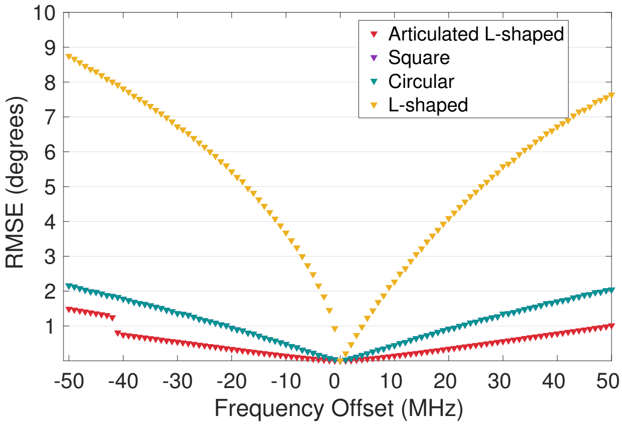

Figure 3.4: RMSE for narrowband signal with Carrier Frequency Offset at SNR = 30 dB

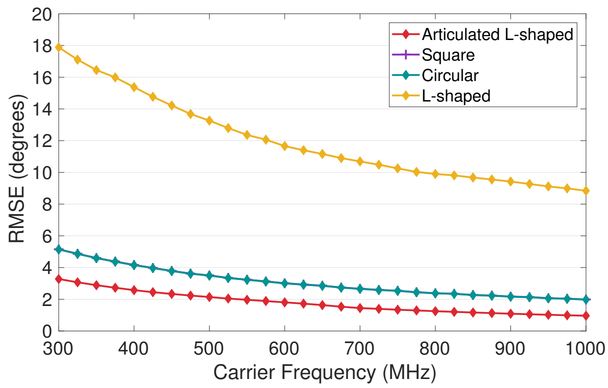

Figure 3.5: RMSE with Frequency Offset 20MHz and SNR = 30 dB

The mean RMSE was then calculated over all possible directions for each offset. In Figure 3.4 the results for SNR = 30 dB are presented. The Articulated L-shaped array exhibits the smallest error, while the circular array and the square array present similar behavior.

For the second experiment the source was placed at the same directions as in the first experiment, and the frequency offset of the incoming signal was set to +20 MHz. The expected frequency was varied from 300 MHz to 1000 MHz. Figure 3.5 presents the RMSE results for 30 dB SNR level. Again the Articulated L-shaped array has the best performance, while the L-shaped array exhibits the greatest estimation error.

The significance of this particular metric becomes evident in scenarios where the incoming signal experiences effects like Doppler. This particular effect, caused by a source moving in high speeds, can result in the signal drifting significantly from its original frequency. This can have a negative effect to the performance of a direction estimation system as this simulation shows. An example for such a system is a satellite ground station equipped with an array of antennas intended to track Low Earth Orbit satellites orbiting in great speeds around the earth. We can see that the Articulated L-shaped array is an excellent option for such scenarios since it is very resilient in frequency offsets in comparison to the rest of the arrays, in addition to using less antennas. Adding to that, such a ground station can be tuned to a single carrier frequency and track multiple satellites operating in a wide bandwidth, without the need to change the center frequency of the array according to the target satellite.

3.1.2.3 Array Size

We further examine the impact the number of antennas has on the performance of the arrays. An increasing number of elements provides grater estimation accuracy with more degrees of freedom, but also increases the cost of the deployment. For this reason a suitable number of elements must be used, that guarantees a certain level of accuracy but at the same time keeps the cost at low levels.

Figure 3.6 shows the results of our experiment. A signal source is placed at $10°$ intervals in the azimuth and elevation planes and the mean value of all estimations is taken. We can see that the articulated L-shaped array has the lowest RMSE across all sizes, while it is also evident that increasing the number of elements per array decreases the estimation error.

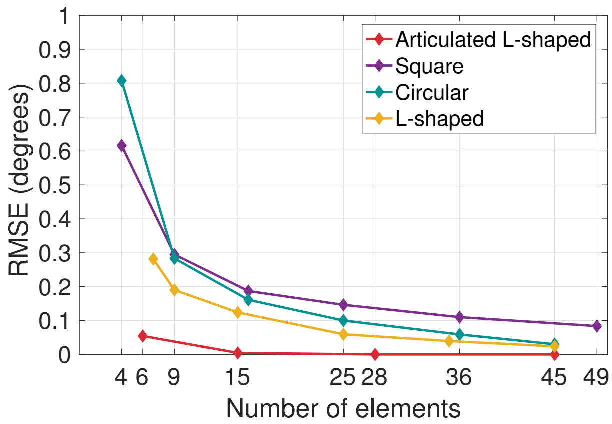

Figure 3.6: Number of antenna elements versus RMSE for DoA $\phi = 85°$, $\theta = 85°$, no noise

The geometry of each array does not allow for using always the same amount of antennas for all arrays for each experiment. The Articulated L-shaped array for example can have explicitly $2 * N^2 - N$ elements in order to keep its geometry intact, where N is the dimension of the Square array on the xy plane. Similarly the L-shaped array must have $2 * N - 1$ elements, where N is the length of the linear array in the xy. To overcome this limitation we tried to keep the number of antennas of the various arrays as close as possible during the experiments.

It is obvious that increasing the number of elements improves significantly the estimation error. That doesn't happen in a linear way though. For all the arrays the results follow an inverse exponential curve which signifies that at some point adding more elements to the array does not lead to significant improvement of the estimation.

3.1.2.4 Spatial acuity

We define the spatial acuity of an array as the capability to distinguish between two signals whose sources are closely located. In our simulations the following assumptions were made: Two signals are considered partially distinguished when each peak corresponding to a signal has a 3 dB margin from the local minima in between them. When that margin exceeds 6 dB, the two signals are considered well-distinguished. In essence we define two boundaries as to when two signals are considered separate and it is at the discretion of the reader to choose which of the two boundaries best fits the application of interest.

Each simulation was run 1000 times at an SNR of 30 dB and Tables 3.1 to 3.4 present the percentage at which each boundary was achieved. We started at 1 degree separation and tested each array configuration up until 5 degrees of separation between the sources. We also tested them for signals on the same azimuth and on the same elevation. The fixed azimuth and elevation angles used were the 45 degrees angle, while the azimuth of the two signals at the first scenario were initially 44 and 46 degrees respectively. The same starting angles were used for the elevation of the signals in the fixed-azimuth scenario.

The L-shaped array cannot easily differentiate between signals coming from the same elevation angle, hence the very bad results in the fixed-elevation scenario. On the other hand it has an excellent performance as far as signals at the same azimuth angles are concerned.

As we can see, the Square array needs 4 degrees separation to be able to distinguish with more than 6 dB between two signals both in the fixed-azimuth and fixed-elevation scenarios, while the Articulated L-shaped array needs 4 degrees separation in the fixed-azimuth and more than 5 degrees separation in the elevation plane to successfully differentiate between two signals. The Circular array performs very well in both scenarios and needs 5 degrees separation between the signals to achieve the 6 dB boundary.

	Fixed Azimuth			Fixed elevation		
Seperation	<3dB	>3dB	>6dB	<3dB	>3dB	>6dB
1°	100%	0%	0%	100%	0%	0%
2°	70%	30%	0%	100%	0%	0%
3°	0%	100%	40%	80%	20%	0%
4°	0%	100%	100%	20%	80%	0%
5°	0%	100%	100%	0%	100%	70%

Table 3.1: Articulated L-shaped array

	Fixed Azimuth			Fixed elevation		
Seperation	<3dB	>3dB	>6dB	<3dB	>3dB	>6dB
1°	100%	0%	0%	100%	0%	0%
2°	60%	40%	10%	60%	40%	0%
3°	0%	100%	90%	0%	100%	50%
4°	0%	100%	100%	0%	100%	100%
5°	0%	100%	100%	0%	100%	100%

Table 3.2: Square array

The Square array exhibits good behavior as far as estimation error in the positive elevation hemisphere is concerned, but fails to successfully detect signals with frequency offset. The L-shaped array cannot differentiate between signals coming from the positive and negative azimuth and exhibits relevantly high estimation error. The Circular array exhibits a very good overall performance and could be a viable option for direction of arrival estimation. The Articulated L-shaped array has the best resilience to frequency mismatch between the expected and the actual received signal, a phenomenon which is

	Fixed Azimuth			Fixed elevation		
Seperation	<3dB	>3dB	>6dB	<3dB	>3dB	>6dB
1°	30%	70%	0%	100%	0%	0%
2°	0%	100%	100%	100%	0%	0%
3°	0%	100%	100%	100%	0%	0%
4°	0%	100%	100%	60%	40%	0%
5°	0%	100%	100%	0%	60%	40%

Table 3.3: L-shaped array

	Fixed Azimuth			Fixed elevation		
Seperation	<3dB	>3dB	>6dB	<3dB	>3dB	>6dB
1°	100%	0%	0%	100%	0%	0%
2°	100%	0%	0%	70%	30%	0%
3°	40%	60%	0%	10%	90%	20%
4°	0%	100%	60%	0%	100%	80%
5°	0%	100%	100%	0%	100%	100%

Table 3.4: Circular array

evident at most real world applications. Also, it shows results close to those of the Square array with regard to estimation error and spatial acuity. At the same time it uses together with the Circular array, the least possible number of antennas, making them excellent choice for low cost deployments.

3.2 Frequency vs Time domain manipulation

An efficient localization algorithm must be in place to recognize the DoAs of multiple sources. In the case of METAL this is particularly important so that multipath reflections are detected and compensated for, and are not regarded as actual transmitting sources. The criteria that must be met for the successful detection of multiple target detection are two: firstly a strong certainty of the maximum or local maximum values of the pseudospectrum corresponding to the estimated sources' DoAs is required in order to avoid ambiguity. Secondly, two closely spaced sources should be distinctively local maximum values, meaning that the pseudospectrum values of the two estimated directions should have as large as possible difference to the local minimum values between them. Essentially this criterion defines that for two signal sources there should be two high and distinct peaks in the spectrum. This concern has led us to investigate the domain on which MUSIC should work so as to achieve the aforementioned criteria, the frequency or the time domain.

MUSIC was initially introduced as a narrowband DoA estimator. Since many of the protocols that METAL could be used in conjunction with use wideband signals, our initial approach was to find a way to adapt MUSIC to such signals. The first idea in applying MUSIC to a wideband signal, namely the OFDM modulated, 20MHz signal of IEEE 802.11b which we used, was to use only a portion of the spectral mask of the signal to perform the estimation. An OFDM symbol of this protocol spans a bandwidth of 20MHz utilizing 64 subcarriers. For each antenna we took the frequency representation of the signals using Fast Fourier Transform (FFT). The next step included selecting one of the subcarriers of the FFT window for each antenna. This subcarrier was used for all consecutive time frames of the captured signal and the MUSIC algorithm was then

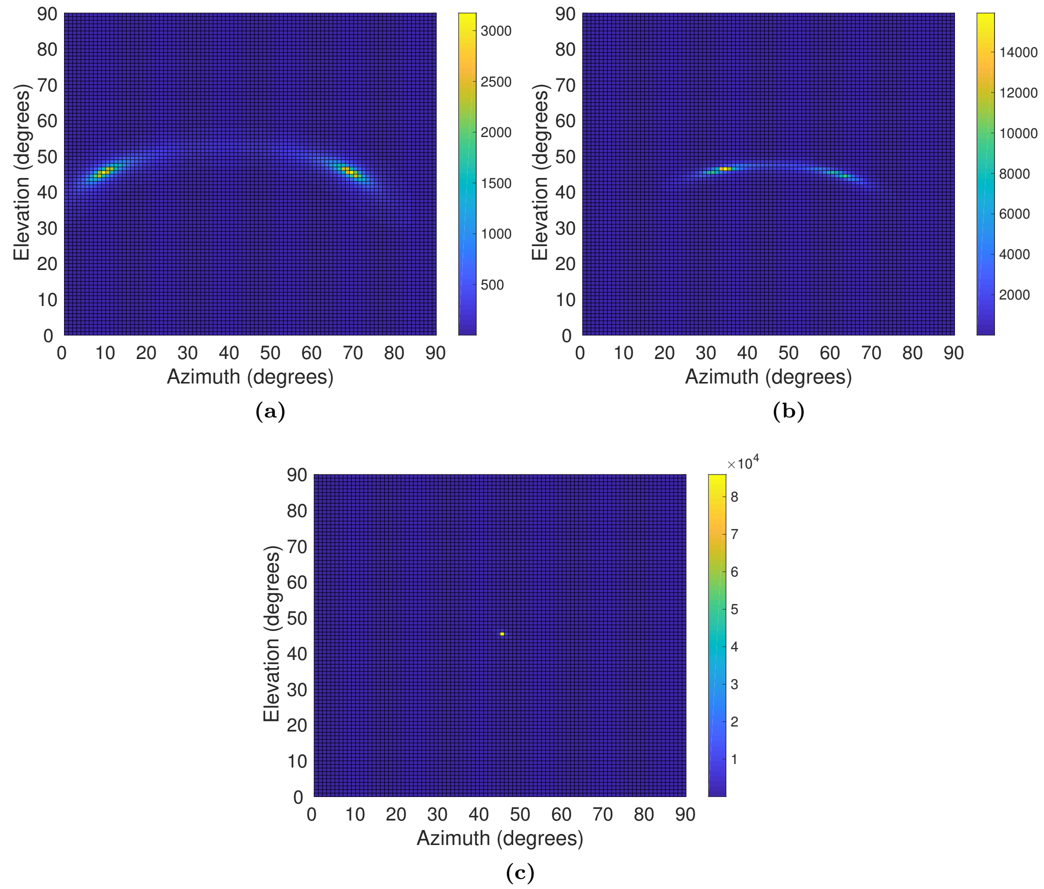

Figure 3.7: MUSIC pseudospectrum for one-carrier utilization with two sources at (az, el) (a) (10°,70°), (b) (30°,60°) and (c) (40°,50°)

executed over that subset of the total frequency spectrum. The steering vector of the Equation 2.7 was calculated for the frequency of the specific subcarrier. This way we acquire a portion of the total frequency spectrum, and therefore a narrowband signal.

In Figure 3.7 the results for three different placements of the sources are depicted. The pseudospectrums of MUSIC are plotted for each of them, with the azimuth plane on the x axis and the elevation plane on the y axis. For the first case in subfigure 3.7a the two transmitters were placed at 10° and 70° azimuth respectively. In the second case in subfigure 3.7b the azimuth direction of 30° and 60° respectively was chosen while for the third case, 3.7c, the sources were placed at 40° and 50° azimuth. The elevation was kept constant at 45°. The SNR of the received signal was set to 30 dB. We can see that MUSIC can distinguish the two sources correctly in the first case since the local maximum values correspond to the real directions of arrival. In the second case the estimated directions are azimuth 34°, elevation 47° for the first and azimuth 63°, elevation 45° for the second source, so there is a small deviation from the true values. In the last case, only one target was identified and that corresponds not to one of our sources, but to the direction in the middle of the two transmitters, namely the 45° azimuth and 45° elevation, where none of our transmitters was placed.

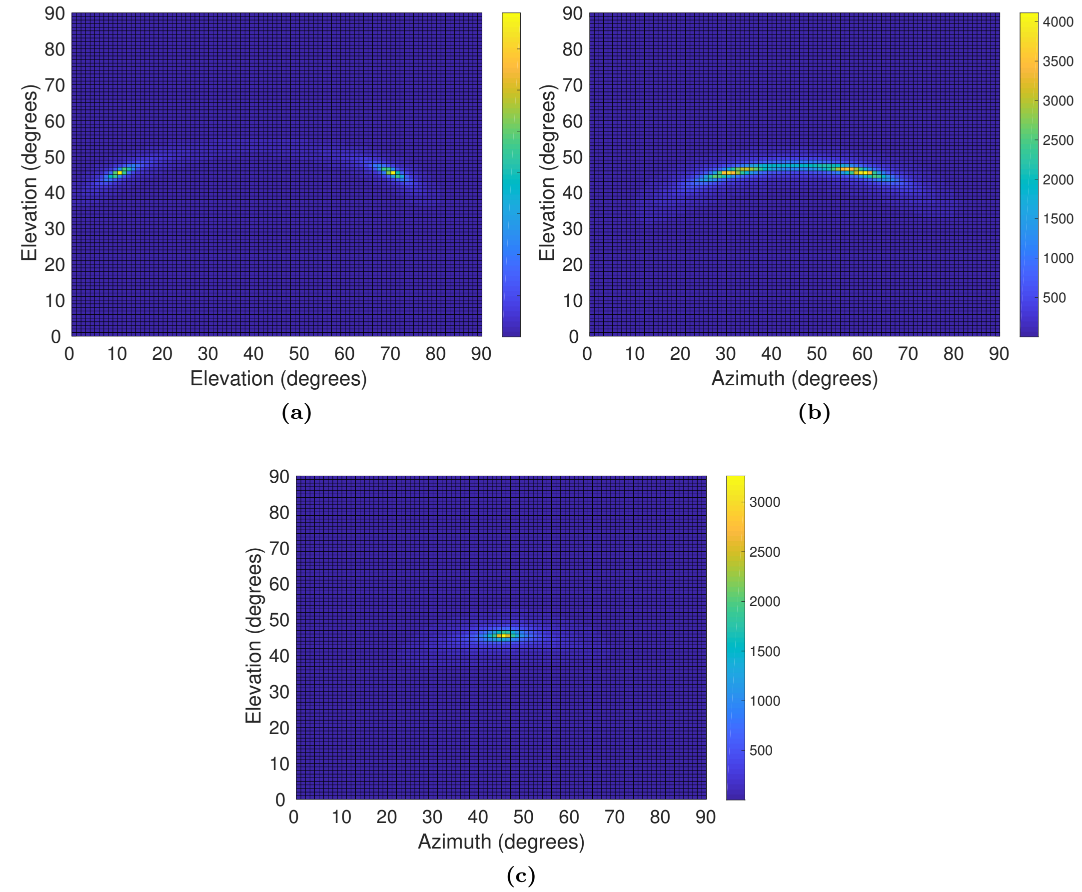

Figure 3.8: MUSIC pseudospectrum for all-carriers utilization with two sources at (az, el) (a) (10°,70°), (b) (30°,60°) and (c) (40°,50°)

It is evident from the previous experiment that even at a high SNR level, the single carrier approach is not able to differentiate between closely located sources, and instead produces a wrong estimation. But even in remotely placed sources, the estimation is not decisive: a large number of high values in the pseudospectrum around the true values is observed. This tells us that the certainty of the estimation is not high, since there are many high values in the pseudospectrum that could also be candidates for the actual DoA.

In an attempt to utilize all available frequencies instead of one, so that the certainty increases, we performed the above process for each subcarrier of the FFT. The MUSIC pseudospectrums for each FFT bin were estimated and were combined, so as to produce the final estimation using the following formula:

$$PS_{final} = \sqrt[nfft]{\prod_{i=1}^{nfft} PS_i} \tag{3.1}$$

where PS_i is the Pseudospectrum for each carrier and $nfft$ is the length of the FFT we

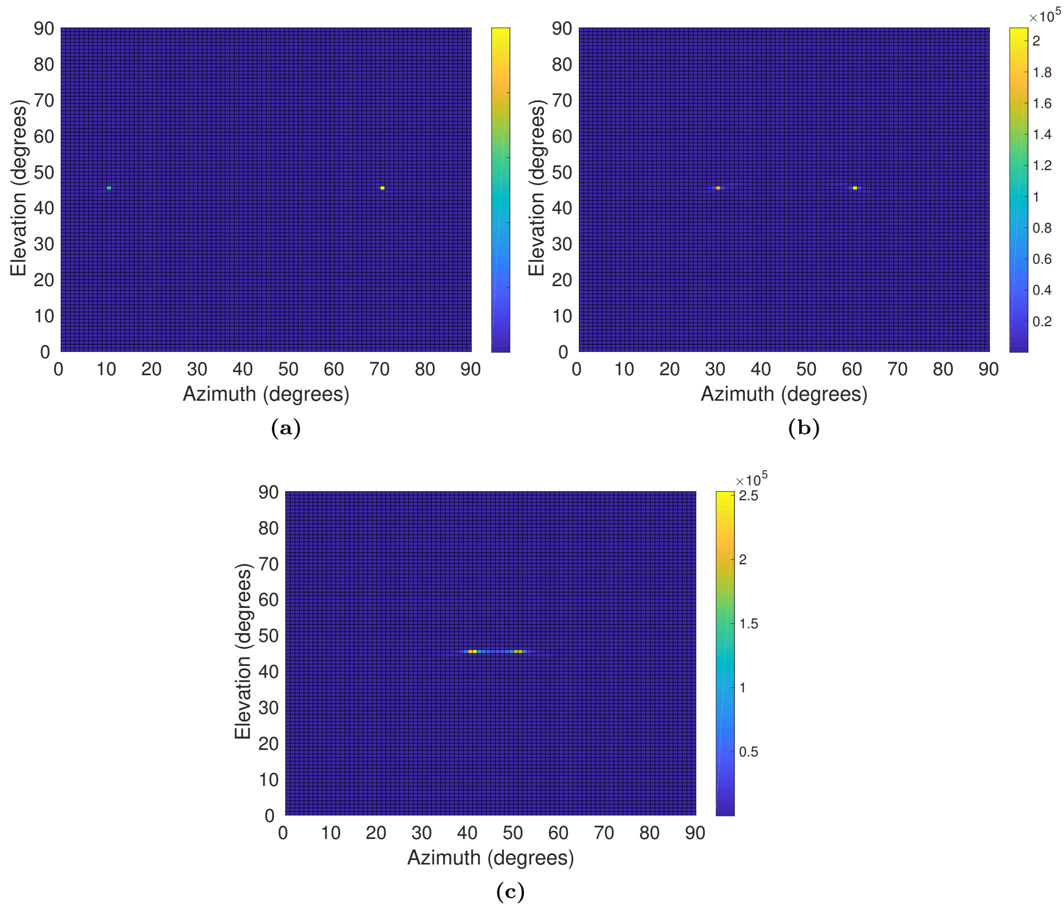

Figure 3.9: MUSIC pseudospectrum for time domain approach with two sources at (az, el) (a) (10°,70°), (b) (30°,60°) and (c) (40°,50°)

performed, hence the number of available subcarriers. For the multiplication we take the dot product of the individual spectrums. The results are presented in Figure 3.8

In the first case of the widely spaced sources, as subfigure 3.8a shows, the estimation has improved compared to the one-carrier utilization. The sources' direction has been correctly identified, with a high and distinctive value of certainty compared to the neighboring cells of the pseudospectrum. When though the separation of the sources decreases, the results are even worse than our first approach. In the second case in subfigure 3.8b there is a high dispersion of significantly elevated certainty values around the true DoAs, although the local maximum values correspond to azimuth values 30° and 70° respectively and elevation values 46° for both sources. For the third scenario, the estimation is again 45° azimuth and elevation, but again with higher dispersion of values than our first approach, as is depicted in subfigure 3.8c.

The frequency approach however neither has the desired performance nor does it satisfy the criteria that we posed in the beginning. As a next approach, we will investigate the case of manipulating the time domain samples. In this case we simply feed MUSIC algorithm with the time domain samples without any other pre-processing. The results are shown in Figure 3.9. In all three cases the sources have been identified correctly, with high certainty and discrete detection of both DoAs even in the 10° azimuth separation in the third scenario. Evidently, the time domain satisfies all the desired criteria for detection of multiple sources and thus, this approach will be used for all subsequent simulations and experiments.

3.3 Array placement

We saw in previous sections that not all directions of arrival are detected as successfully, especially in the presence of noise. Since our system uses two arrays to infer the user's location, an important parameter is the placement of the arrays in space. The two should be in such a formation, that a 'blind-spot' direction for the one, is a clearly detected one by the other, so that the total error is minimized.

We tested various formations, assuming 6 element articulated L-shaped arrays, in order to simulate a realistic, low-cost scenario, in a rectangular room of 10x20 meters. In Figures 3.10 and 3.11 the different formations that we tested are depicted. Initially we placed the two arrays on the same wall. As can be seen in Figure 3.10, each line connecting two dots, labeled A1, A2 to A10 and B1 to B5, is one formation that we tested. The concept is that for each wall, one of the two with the smallest dimension and one of the walls with the greatest dimension, we place firstly the arrays at an equal distance of one meter away from the middle of the wall, and then for each consequent formation we place them one meter further apart towards the edges of the wall. This gives us ten different formations for the big wall, and 5 for the smaller. For each formation we placed a source at each point in the room, with one meter intervals. Furthermore, we assumed two scenarios for each test: in the first, the arrays are on the same level will the transmitters, while in the second the plane of the transmitters is 1.5 meters higher than the plane of the arrays. This way we also evaluate the placement of them, in height. In Figure 3.11 three more cases that we tested are depicted. In the case labeled O1 the arrays were placed in the middle of the two longest walls, in the O2 case they were placed in the middle of the smaller walls, while in the O3 case one array is placed in the middle of the larger wall and the other is on the corner of the room, with their junction creating a right triangle with the two walls.

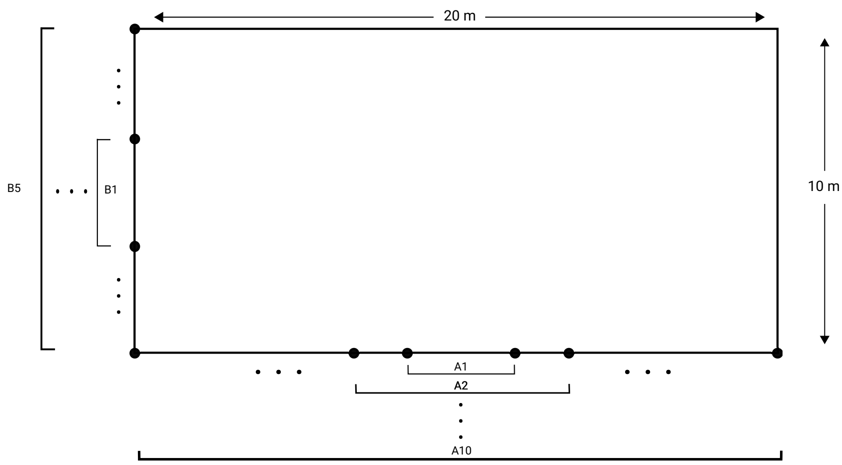

Figure 3.10: Experimental placement of arrays on the two walls

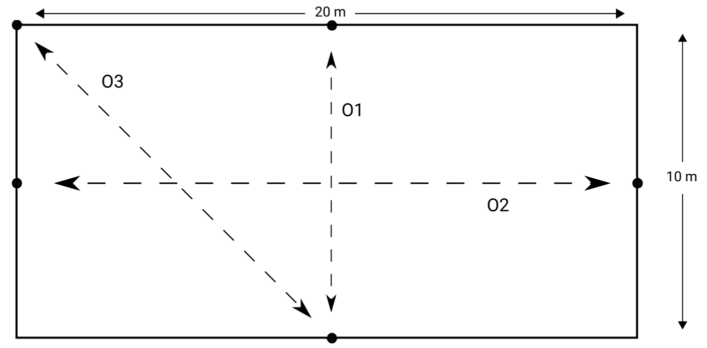

Figure 3.11: Experimental placement of arrays in various extra formations

Tables 3.5 summarizes the results. The mean RMSE was calculated for each formation over the RMSEs of each position of the source in the room using the formula

$$meanRMSE = \frac{\sum_{p=1}^{N} RMSE_p}{N} \tag{3.2}$$

where N is the total number of sample positions. In the case of the array plane being the same with the users plane, the most suiting placement is the A1 scenario, while in the case of .15m distance between the planes the placement of scenario O1 has the best performance.

3.4 Multipath and ITU model

The International Telecommunications Union (ITU) [28] has issued guidelines for evaluation of transmission technologies [29]. These guidelines will help us evaluate our system in the presence of multipath reflections. In the recommendation, a channel impulse response model is given and it is based on a tapped-delay line. In essence, the output of the channel is described as the superimposition of a direct path signal and multiple delayed and attenuated versions of it, using the formula:

$$y(t) = \sum_{n=1}^{N} w_n * x(t - t_n) \tag{3.3}$$

where w_n is the attenuation of the path n, t_n the time delay relative to the first path, and $x(t)$ the original signal. Furthermore, not only one but two multipath channels are defined. This derives from the fact that the delay spreads can vary occasionally, resulting to much larger spreads that the majority of the time. In order to evaluate successfully the desired parameters, these occasions must also be taken into account. For this reason a second "worst-case" channel with larger delay spreads is also defined. The parameters of the two channels are presented in Table 3.6

These are the two channels which will be used in the evaluation of our system. We consider them as the ground truth since they have been published by the ITU. The above channel model does not include the angles from which each path arrives at the receiver. For that reason we suppose that the reflected signals arrive from random elevation and

	Plane distance 0 meters		Plane distance 1.5 meters	
Scenario	**5 dB**	**30 dB**	**5 dB**	**30 dB**
A1	3.72	1.99	4.43	0.43
A2	6.3	2.89	0.67	0.27
A3	3.96	3.78	0.44	0.24
A4	49.9	3.34	0.58	0.23
A5	10.7	4.6	0.64	0.23
A6	13.2	6.22	0.62	0.64
A7	8.12	9.1	0.70	0.22
A8	11.79	8.09	0.59	0.22
A9	13.15	7.63	0.87	0.23
A10	15.28	10.24	1.09	0.26
B1	11.62	2.8	5.22	1.99
B2	9.96	3	6.04	2.89
B3	17.9	3.8	5.40	3.78
B4	12.22	6	5.64	3.34
B5	10.87	4.6	6.3	4.59
O1	4.77	3.38	0.15	0.16
O2	12.34	8.63	1.39	0.26
O3	4.84	7.93	0.75	0.21

Table 3.5: Mean Estimation Error of examined array placements

	Channel A		Channel B	
Path	Relative Delay (ns)	Average power (dB)	Relative delay (ns)	Average power (dB)
1	0	0	0	0
2	50	-3.0	100	-3.6
3	110	-10.0	200	-7.2
4	170	-18.0	300	-10.8
5	290	-26.0	500	-18.0
6	310	-32	700	-25.2

Table 3.6: ITU indoor channel model

azimuth angles. Furthermore, ITU specifies that the delay of the paths can be adjusted $\pm 3\%$ to match the sampling rate of the system. Since we will use METAL over the IEEE 802.11, the sampling rate is 20 MHz and we will adjust the delays accordingly to be multiples of 50 ns, i.e. the time duration of one sample for the given sampling rate.

3.5 Evaluation of Localization System

In this section we evaluate the performance of our algorithm. The metric, most indicative of a localization system's performance, is the mean estimation error, i.e. the deviation of the actual position from the estimated one. Our simulations are carried out assuming a room with dimensions 20m x 10m as in section 3.3. As we saw in the same section, the most efficient placement for the two arrays of our system is for each one to be placed in the middle of the largest wall, in order to have the smallest RMSE. Furthermore, the plane of the arrays must be at a higher level that the plane of the users, as being on the same plane deteriorates performance, according to the results of section 3.3. For this reason we will assume a difference of 1.5 m between the two planes, with the plane of the arrays to be the highest.

Next we create a path for a user which we will use for estimating the mean error. The path as well as the setting of the room and the arrays is depicted in Figure 3.12. The positions at which an estimation is taken are denoted with x. At each of those positions a number of snapshots are taken from each array and are used for position estimation. The geometry of the arrays will be determined through simulations in Section 3.5.1, since intuition tells us that different geometries will have different estimation performance. The SNR of the received signal is set to 10 dB for all cases.

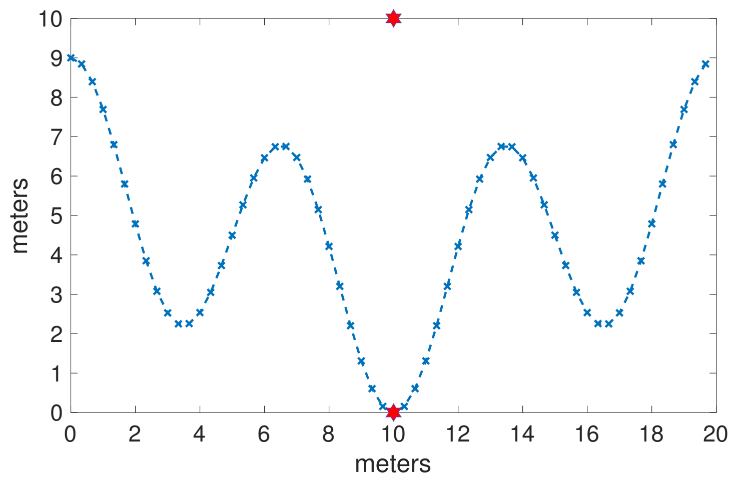

Figure 3.12: Arrays placement and selected user path for evaluation

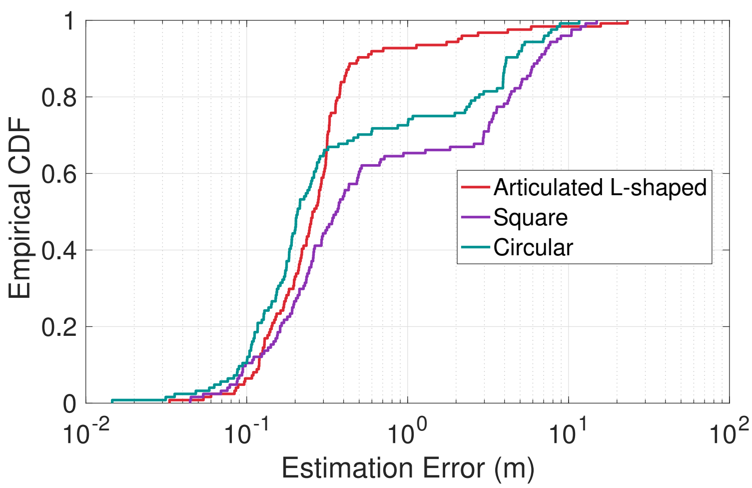

Figure 3.13: Array Performance

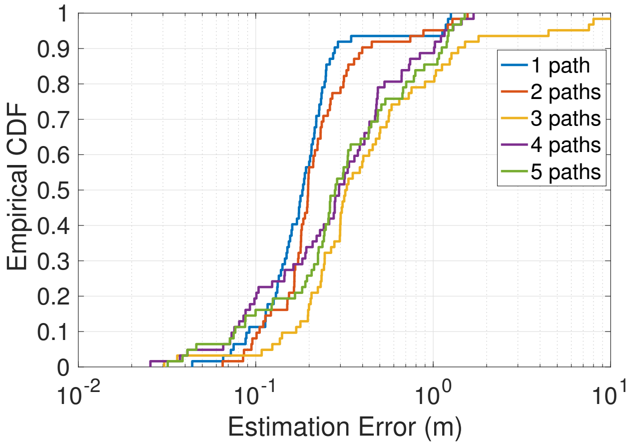

(a)

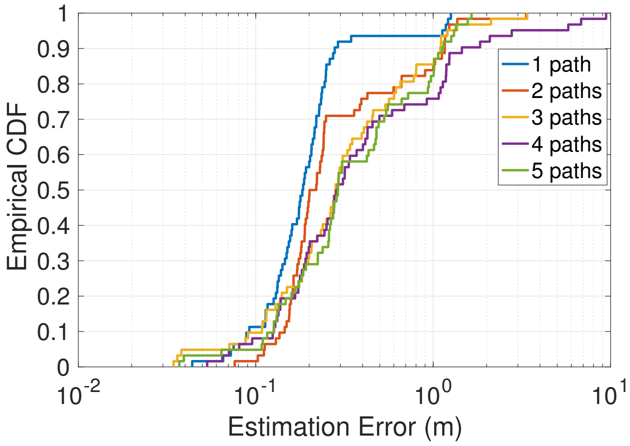

(b)

Figure 3.14: CDF with and with different amounts of multipath components for (a) Channel A and (b) Channel B

3.5.1 Error vs Type of Array

In an attempt to select the most appropriate array geometry for our system, we simulated the performance of different arrays in the context of our system, and specifically the arrays we examined in our array evaluation in Section 3.1. In Figure 3.13 the results of the simulations are depicted. The Articulated L-shaped array presents the highest performance since it has an 80^{th} percentile at 0.8m while the square and circular array present over 3m estimated error at the same percentile. The median error is at 0.3m for all geometries. For the rest of the simulations the articulated L-shaped array will be used.

3.5.2 Error vs Number of Multipath Components

Next we evaluate the system in the presence of different number of multipath components in the received signal. Figure 3.14 shows the results for channels A and B of the ITU model. As expected, the estimated error increases as more reflected signals are added to the overall received one. The median error for both channels is around 0.2 to 0.3 m, while the 80^{th} percentile error is increased to 0.6 m, from 0.3 m when more than 2 components exist in the signal for channel A, while for channel B the error at the same percentile is over 0.6 m when one or more multipath components are present. For the rest of the simulations both channels will be used, each one present for 50% of the simulation time.

3.5.3 Effect of outlier detection

In Section 2.4.3 the outlier detection algorithm was described. Its purpose is to decrease the number of outliers, i.e. position estimations that fall far from the range of expected positions and therefore their distance from the actual position is very large. Figure 3.15 depicts the effectiveness of the algorithm. Until the 80^{th} percentile the system performs the same with or without outlier detection. The difference is evident in the higher percentiles, where the outlier detection algorithm has removed the outlier estimations and therefore has improved performance over the case where the algorithm is not used.

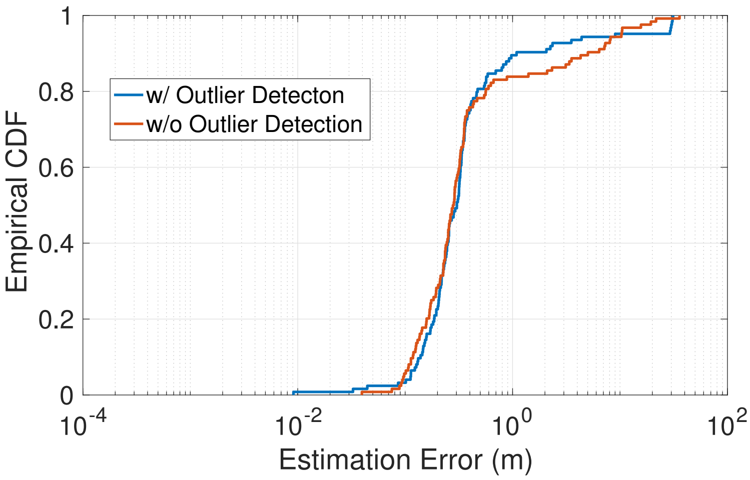

Figure 3.15: Outlier Detection Performance

3.5.4 Effect of SNR level

Next we examine the role the SNR level plays to the estimation error. The results are summarized in Figure 3.16. The performance is similar across all SNR levels,something which is indicative of the high accuracy of MUSIC even in low SNR. There is a drop in performance at the higher percentiles of the 15 dB scenario. This is due to the fact that as the noise level becomes lower, the presence of the reflected components becomes more prevalent in the overall signal, causing MUSIC to detect them more often than in the case of higher noise levels. This leads to mistaken detection of the reflected component as the direct path, and ultimately a failed estimation of the position of the user,which is evident in the higher percentiles of the CDF.

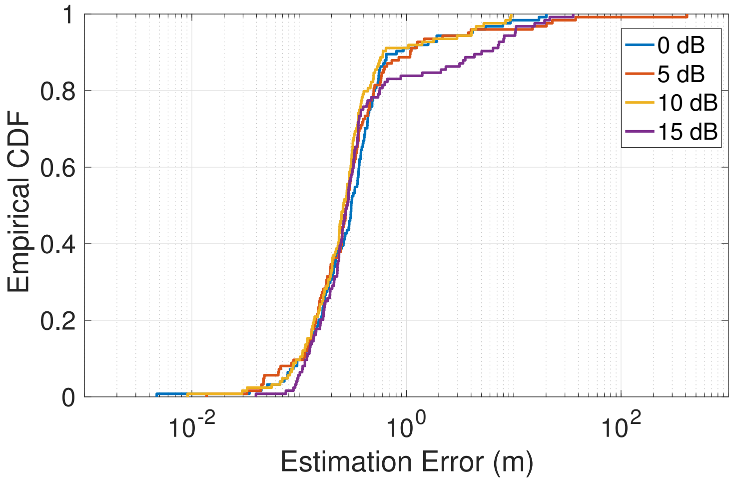

Figure 3.16: Error vs SNR level

Chapter 4

Real Time DoA Prototype

In this chapter we present our real-time DoA estimation prototype system. It is implemented using SDRs, flexible and reprogrammable RF transceivers, who implement DSP functions in software. Below we describe the main aspects of the system

4.1 Software Defined Radios

Traditional hardware radio devices implement the entirety of a communications protocol on hardware chips, making it very costly or sometimes impossible to perform an update on the system, e.g. after a new revision of the protocol. Each device also, implements only a limited number of protocols and in most cases only one. This makes the support of a multi-protocol environment almost unfeasible.

SDRs are programmable communication devices which can be used for various applications and over a very wide range of frequencies. The main advantage over existing hardware radio solutions is that they use a generic RF frontend which provides the captured signals from the medium and all subsequent signal processing functions can be implemented in software. This characteristic makes them an exceptionally attractive solution for many applications that require adaptation to a wide range of protocols and RF frequencies.

4.1.1 Hardware

A general view of the hardware architecture is depicted in Figure 4.1 . The RF frontend consists of the RX and TX antennas, the Up and Down-Converters, the Analog-to-Digital and Digital-to-Analog Converters and the required analog filters. The communication protocol between the device and the host is usually implemented on an Field Programmable Gate Array (FPGA) or a General Purpose Processor (GPP). Other components that can be employed is a Clock Source providing a clock signal for sampling at regular intervals or a GPS Disciplined Oscillator for synchronizing the internal clock with that of GPS, providing a reference for time-sensible applications.

As we've shown MIMO systems offer attractive features to communication applications. Many Software Defined Radio boards incorporate MIMO support for that reason. An SDR board can accomodate MIMO functionality in one of two ways: The motherboard can support multiple plug-on daughterboards which serve as the RF frontends of the MIMO setup. The most novel SDR solutions like Ettus Research's B210 [30] utilize specialized hardware - in the case of B210 the AD9361 chip of Analog Devices - to provide 2x2 MIMO.

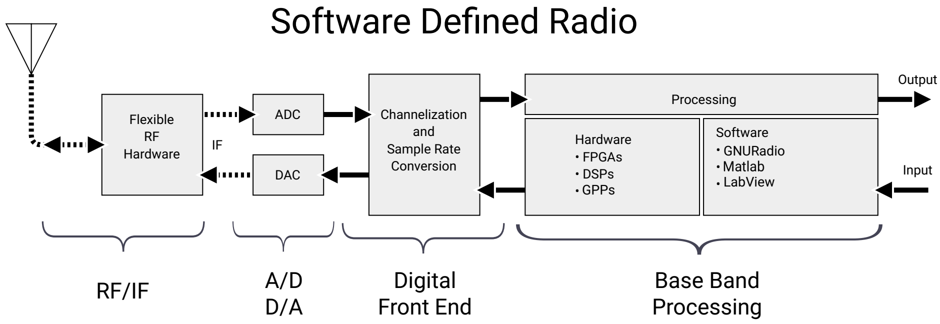

Figure 4.1: SDR architecture

4.1.2 Software

After the baseband samples are retrieved by the hardware, the signal processing is implemented on software. This is the most delicate part of the process, since the real-time demands of communications systems require the most efficient software implementation of signal processing components. The execution of the software routines takes place either on a GPP or a Graphics Processing Unit (GPU) on the host computer. Lately in an attempt to further reduce execution time, the FPGA on the SDR is utilized for executing part of the signal processing functions, something which speeds up significantly the process.

One of the most popular Digital Signal Processing Platforms is GNU Radio. GNU Radio is an open-source project providing great flexibility in designing and implementing software defined communications systems. It follows the principle of block programming and provides wrappers for many time-consuming functions such as Fourier Transform or various filters. Furthermore it makes use of SIMD instructions using a library called Vector-Optimized Library of Kernels (VOLK). This feature reduces the execution time of processes which have greater time overhead. The truly groundbreaking feature of GNU Radio though, is the ability to write custom blocks of code according to the needs of the intended application. A typical GNU Radio signal processor is called a flowgraph and contains all the necessary functions for the signal manipulation in the form of software blocks, as is depicted in Figure 4.2

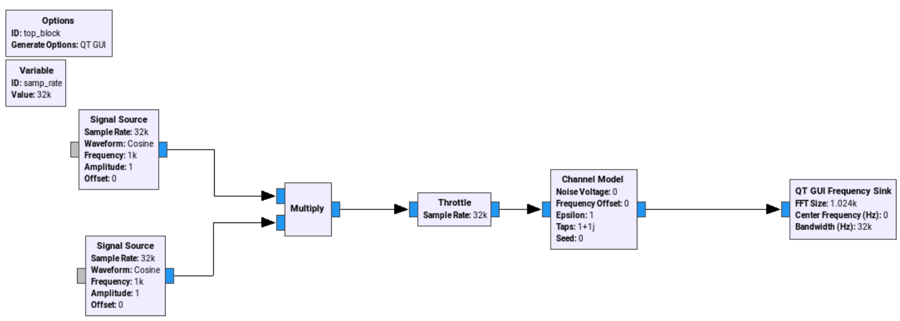

Figure 4.2: GNURadio flowgraph

Some of the advantages that derive from the use of SDRs are:

- **Easier, faster and low cost adaptation of systems to new updates**
- **Support for multi-protocol systems**
- **Ease of testing and debugging**

These traits do not come without drawbacks too. The implementation of signal processing in software requires a lot of CPU resources that are not always available. The use of SIMD instructions reduces the computational cost but other optimization techniques must take place, especially in scenarios where large bandwidths are required. The evolution of multicore processors is a promising factor for future systems as far as latency is concerned. Also the implementation of part of the process flow on the FPGA can significantly help towards achieving the real-time requirements of communications systems. Finally, GPUs have emerged as a promising platform for signal processing because of the parallel programming capabilities they offer.

4.2 Composite Antenna Array

An antenna array is comprised by multiple antenna elements forming a certain geometry which can span from one to three dimensions. The number of receiving antennas by each SDR can vary. More supported antennas usually comes with higher per-device cost. The devices we used, Ettus Research USRP B210, only support two receiving channels. As we needed at least four receiving channels for our array, we had to combine multiple devices for its construction.

As we described in Chapter 2, when using multiple receiving channels in the context of MIMO, frequency and phase synchronization must be ensured beteween the channels. Most SDR hardware that employs MIMO satisfies the above requirements for the different IQ streams, since on one SDR board the same sample clock is used for all streams, making them synchronized in frequency and time. The problems arise when multiple boards are used for a MIMO application. Such a system is very difficult to be used for MIMO applications without preconfiguration. Especially in the area of direction of arrival estimation, even a small deviation from perfect synchronization between the streams of the different boards can cause significant drift from the real direction of arrival. The non-ideal nature of SDR devices poses challenges to the implementation of such applications.

4.2.1 Frequency synchronization

Most distributed systems as well as traditional telecommunications between a sender and receiver suffer from the problem of Carrier Frequency Offset (CFO) between the local oscillators of different devices. This is acceptable up to a level of offset since most communication protocols take this fact into consideration and compensate through various mechanisms. Direction estimation systems must also ensure frequency synchronization in case multiple devices are used, otherwise the estimated angles can fall far away from their true values.

Suppose that we need to use two SDR devices for a direction finding application, each with two receiving antennas. The CFO between different Local Oscillators (LOs) can range from a few Herz to even a few thousand Herz. The effect of the CFO will be a constantly alternating phase offset of the streams of one device relative to the streams of the other. That phase offset will be $e^{j2\pi\Delta ft}$ where Δf is the CFO. MUSIC takes advantage of the phase information existing in the receiving streams. Since the relative phase between

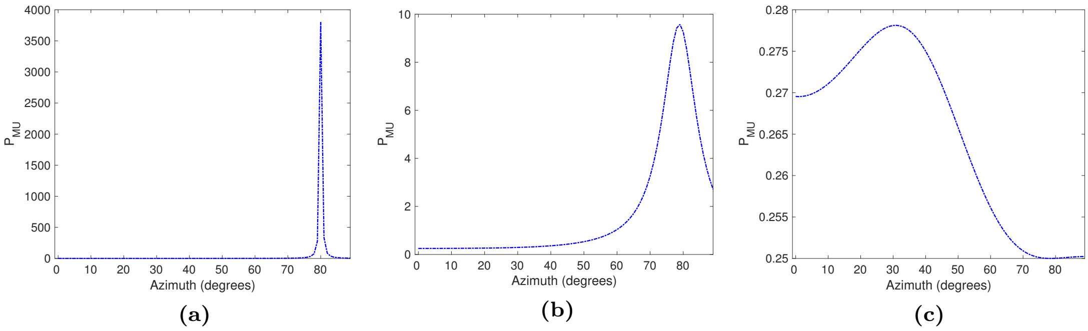

Figure 4.3: MUSIC estimation at time, (a) 0 seconds, (b) 50 nanoseconds, (c) 500 nanoseconds

the streams constantly changes, this will be reflected on the information exploited by the algorithm in a way that will constantly change the estimated angle. For this illustration we will suppose a CFO of 100 Herz. Figure 4.3 shows the effect of the frequency offset on the estimation of a signal originating from a stationary source transmitting from azimuth direction of 80°. The relative phases between the receiving streams are the same at the start of the observation. In graph 4.3a the estimation for time $t = 0$ is shown. Because the relative phases of the streams are the same we get a definitive and correct estimation of the angle of arrival. After 50 ns the phase offset has taken its toll on the estimation which now starts to decline, both in certainty and in accuracy as is depicted in graph 4.3b. After 500ns the result of the estimation is far from the true value of the angle as graph 4.3c. In fact the estimated angle will rotate around the observation space at a rate of $1/\Delta f$ seconds.

The way that most commodity SDR devices deal with this kind of problem is by providing a reference input for synchronizing the LO with an external reference clock. The simplified schematic of an Ettus Research USRP device is depicted in Figure 4.4. The external clock connects to the Reference Input. The clock usually generates a sinusoid which goes through a PLL for phase locking, the output of which feeds the Voltage Controlled Oscillator that eventually drives the internal clock of the device. By attaching multiple devices on the same external clock we can achieve frequency synchronization since all LOs will be driven by the same clock.

4.2.2 Phase Synchronization

Phase or time synchronization is needed for counteracting the inconsistency between the sampling time of each device. This inconsistency adds a constant relative phase offset between the streams of different devices and consequently degrades the performance of a DoA estimation system since the phase offset caused by the relative position of the source and the array which is exploited by the estimation algorithm will be polluted with an extra arbitrary phase offset.

A two-step approach is used for phase synchronization by first performing coarse and then fine synchronization. Since phase is inherently related to time, a phase offset between two channels can be counted in samples, but also a sub-sample offset may be present, which due to insufficient sampling rate can not be depicted in samples. The coarse synchronization attempts to correct the greatest portion of that phase offset, at a sample level. The portion of the offset that is smaller than a sample is compensated through the fine synchronization.

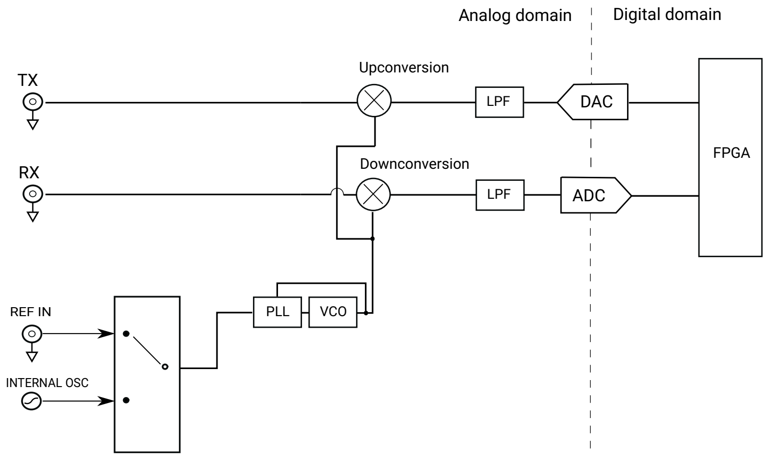

Figure 4.4: USRP schematic

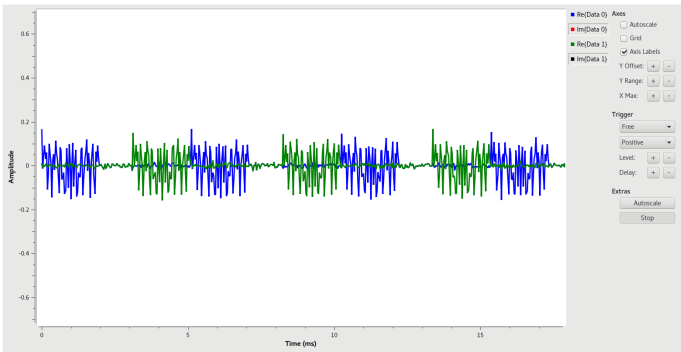

Figure 4.5: Initialization offset of 100 samples for two devices

The largest portion of the phase offset is introduced by the operating system of the host computer. Due to kernel scheduling one device may begin sampling the medium at an earlier time instant than the other devices that may be attached to the same host. This means that one or more streams will contain more samples than the rest. The samples of all streams when reaching the intended application will appear like they have been sampled at the same time. This will not be the case though for the device that was initialized first, since the samples at the beginning will have come from an earlier time instant than those of the streams of the other devices. In Figure 4.5 a signal is arriving from 90° azimuth which means the signal should appear at the same time instant for both streams, each from a different device connected to the host computer. Due to serial initialization of the devices by the operating system, an offset of 100 samples is introduced to the streams. The second device's stream, colored in green, has received more samples at the beginning than the first device. The samples are superimposed at the application, meaning that the excess samples are appearing as if they arrived at the same time instant as the later ones. In this depiction the signal should appear at the same time instant in the two streams, but the excess samples of the one stream have delayed it introducing a phase offset which implies a different angle of arrival than the true one.

The remaining overall phase offset due to timing is due to the sampling clocks of the devices. After we've ensured that the interval of the sampling clocks will be identical through the frequency synchronization, the next issue is the time instant the devices sample the medium which must also be identical otherwise an unwanted phase offset will be introduced in the received signal. This is evident in Figure 4.6, where the sampling clocks of the two devices have an offset of 0.5 radians. This will introduce a phase offset of $e^{j\phi}$ where ϕ is the sampling time offset.

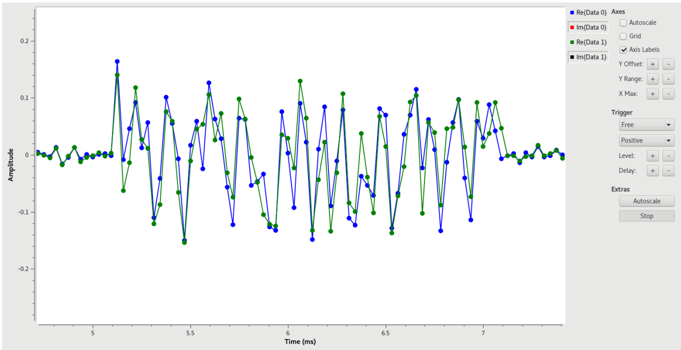

Figure 4.6: Sampling time offset of 0.5 radians for two devices

Taking into consideration the above phenomena, the overall phase offset between the receiving streams of two devices can be described mathematically as

$$\Phi = e^{j2\pi F\Delta t} + e^{j\phi} \tag{4.1}$$

where F is the carrier frequency, Δt is the time offset between the initialization of the devices and ϕ the sampling time offset.

4.2.2.1 Cross correlation with known sequence

The above mathematical formulation suggests that the introduced phase offset could be compensated for, electronically. If the phase offset is calculated for each stream and applied again with opposite sign, then its effect is reversed, since all streams will be synchronized in time. The approach towards estimating that offset is to transmit a known signal and attempt to detect it in all streams. Then by calculating the time difference of arrival between them we can align the samples and phases accordingly so that all of them become synchronized.

For our implementation we used the long training sequence of the IEEE 802.11b protocol. The protocol uses a short training sequence for coarse synchronization and a long training sequence for channel estimation and fine frequency synchronization. The rationale behind this selection is that it's been used in a widely applied and successful protocol with high performance in achieving fine frequency synchronization. Adding to that is that cross-correlating a signal containing the sequence with the sequence itself provides distinctive peak values in sample level, enabling us to accurately detect in time the presence of it in the received signal of all streams and compensate for any existing phase offset.

The cross-correlation function is implemented in GNU Radio by the FFT filter block in Figure 4.7. This block takes the receiving stream as input and the long training sequence in time as an argument and produces the output according to the function

$$out = ifft(fft(in) * fft(long\_sequence)) \tag{4.2}$$

Figure 4.7: FFT filter block

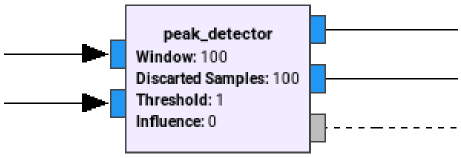

Figure 4.8: Peak Detector block

The output is a time series with peak values at the time instant of detection of the sequence. In Figure 4.9 the input and output of the block are illustrated. We can see that the end of the sequence in time domain gives a distinct peak value at the output of the filter.

4.2.2.2 Peak detection

The peak values of the output of the FFT filter block for each stream must be detected in order to identify the delay induced by the initialization time of each device. This way the Δt of Equation 4.1 and hence the first term of the overall phase offset will be evaluated. This is the work of our peak detector block, depicted in Figure 4.8. In essence this block counts the number of samples between each detection of the long training sequence at the various streams.

The algorithm initially discards a number of samples from each stream after initialization to avoid some spikes which are sometimes observed at the initial samples of a capture. The number of samples to be dropped are specified through the corresponding argument. Then a noise floor value is computed for each stream which is actually the median value of a number of samples specified by the 'Window' parameter. After this value has been calculated, the median value of the input samples is computed. The determination of whether a value is peak or not is a combination of a user defined threshold and the median

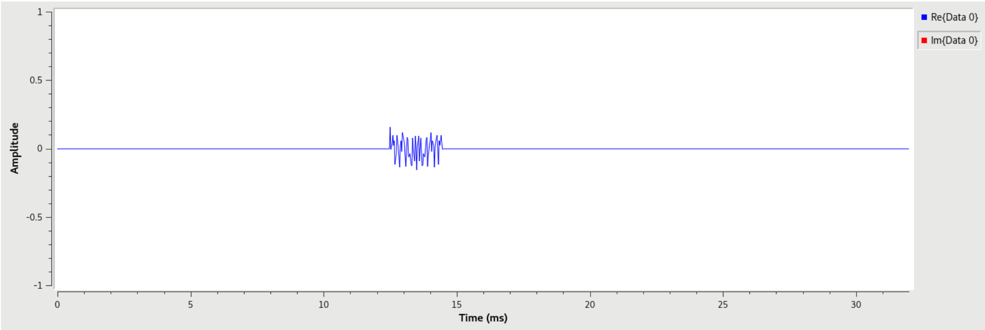

(a)

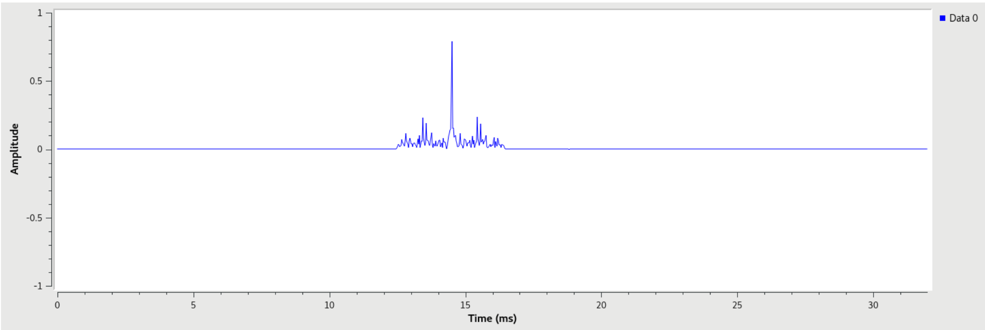

(b)

Figure 4.9: FFT filter, (a) Input and (b) Output

value computed from the past samples. When the first peak is determined for a stream, a counter is initiated until a peak is also detected for the last stream. This last stream is considered a reference, and the sample difference of the reference stream to the rest is passed on to the block handling the alignment of the samples through a message queue.

At the same time the peak detector block holds the peak value for each stream in order for the aligner block to perform fine time synchronization i.e. determine the last part of Equation 4.1 by estimating ϕ. To do that we calculate the angle of the peak value for each stream using the $atan2$ function. We set ϕ equal to that angle. We know that the ideal peak value of the cross-correlation output is at $0°$. Any other value for the angle would indicate a non-ideal time instant for sampling by the device. By calculating the angle and multiplying each stream with its corresponding $e^{-j\phi}$ we manage to electronically align the sampling instants of the devices by using the $0°$ angle for the peak value as a reference. In Figure 4.10a the ideal complex output is depicted while in Figure 4.10b the result of the signal sampled at a non-ideal time instant is in the form of a phase-shifted cross-correlation output. The real (blue color) and imaginary (red color) parts of the complex stream is plotted in both graphs.

in Figure 4.11 the complete synchronizer flowgraph is depicted. Two USRP B210 devices are used in this flowgraph, each with two receiving antennas. The inputs are forwarded to the FFT filter blocks for the cross-correlation with the known long training sequence and to the aligner block which will align the samples properly after detection of the sequence. The output of the filters are then normalized in order to compensate for any possible gain mismatch between the antennas which would degrade the ability of detection by the peak detector block. When the sample offset as well as the phase offset

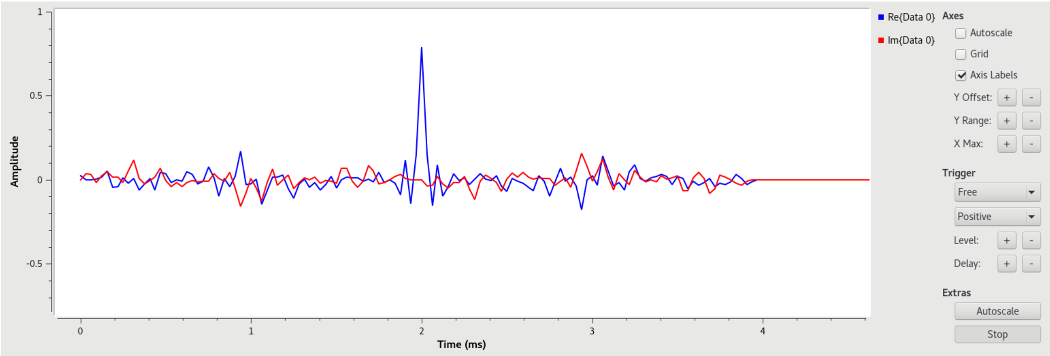

(a)

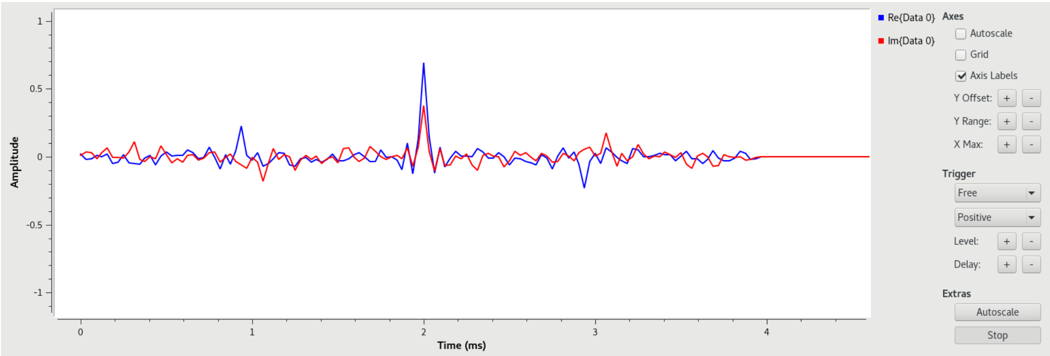

(b)

Figure 4.10: Complex cross-correlation output, (a) Ideal and (b) Phase-shifted

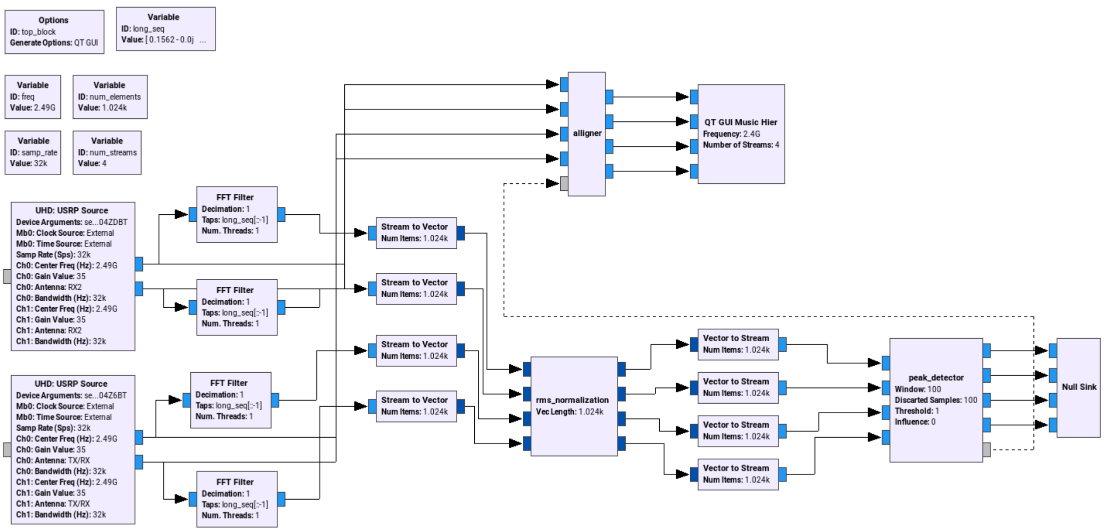

Figure 4.11: Synchronizer

are calculated by the peak detector, this information will be passed to the aligner block which will eliminate the aforementioned offsets and achieve time synchronization which is necessary for the MUSIC to accurately estimate the DoA of a transmitter.

Figure 4.12 shows the percentage of successful detection of the long training sequence with the cross-correlation function. For each SNR level we examined whether the peak value was detected at the correct sample of an observation window. It is evident that even at -12 dB SNR the long training sequence is always successfully detected, making this technique reliable even at negative SNR.

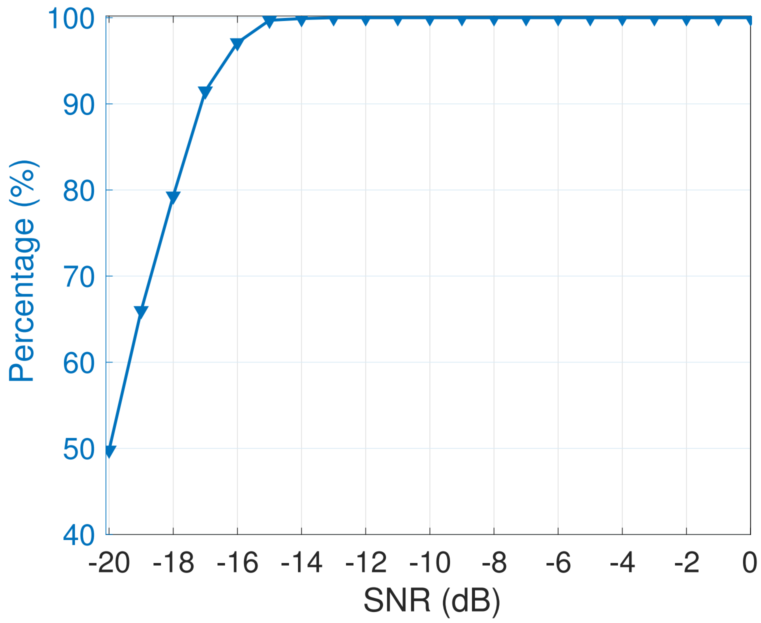

Figure 4.12: Long training sequence detection success

4.2.2.3 Samples per Snapshot

MUSIC algorithm takes as input a number of samples and produces one estimation for the DoA of a signal. Each set of input samples is called a snapshot. The selected amount of samples per snapshot has an effect on the accuracy of the estimation, which is depicted in Figure 4.13. Increasing the sample set size yields lower RMSE. At the same time, as Figure 4.14 shows, the bandwidth that can be observed increases and the number of estimations per second decreases, since more samples are consumed for one estimation.

It is important to notice the decrease in achievable bandwidth above 8192 samples per estimation, as well as the low achievable bandwidth for lower number of samples per snapshot. The latter is the result of greater computational overhead at the medium-performance PC that we utilized for our experiments (Intel i5-3470, CPU @ 3.2 GHz). The Singular Value Decomposition required from MUSIC has greater overhead as the size of the sample set increases, which causes less samples per second to be consumed and hence, smaller bandwidths observed. On the other hand, smaller sample sets also lead to smaller achievable bandwidth due to the fact that more memory copies take place in the GNURadio platform, which also lead to increased overhead.

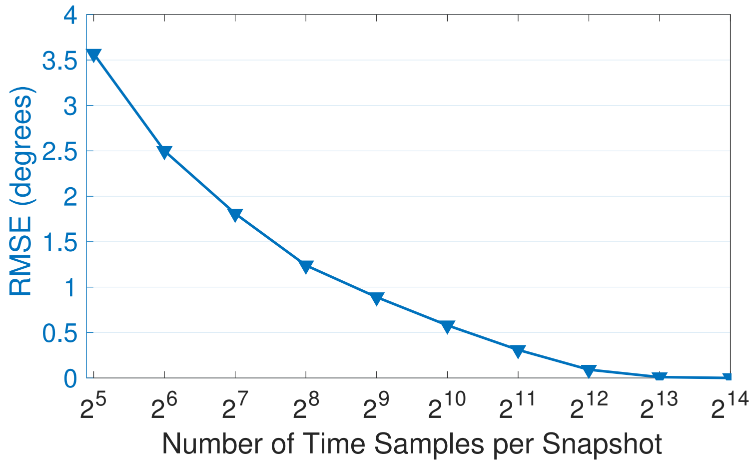

Figure 4.13: Number of time samples vs RMSE

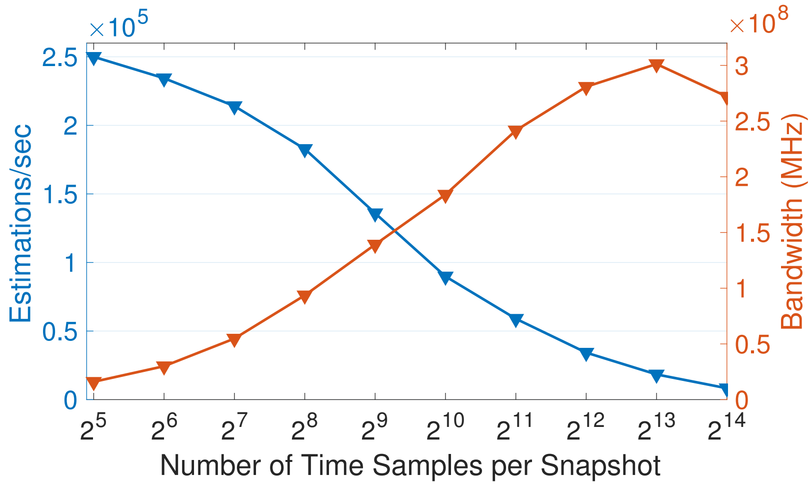

Figure 4.14: Number of time samples vs RMSE and achievable bandwidth

Chapter 5

Conclusions

In this work we presented METAL, a localization system which can be used together with a wide range of telecommunication protocols, for target position estimation. METAL employs the MUSIC algorithm for DoA and makes use of a phased antenna array. The system uses the mechanisms of a protocol to its benefit, with the goal of improving the accuracy of the estimation. The medium access control mechanism that many protocols employ in order to regulate the access of the users to the medium can be exploited to achieve per-user signal detection and therefore position estimation. The training sequence used for synchronization of the packets of the protocol, if present, can help us identify the angle of arrival corresponding to the direct path signal component in a multipath rich environment.

For proof of concept of our system we utilized SDR devices, which provide great flexibility. We were able to compare the use of time and frequency samples in the estimation process of the MUSIC algorithm, and come to the conclusion that time samples manipulation offers the greatest accuracy. For the needs of our system we also had to construct the phased array using multiple SDR devices. During this process we faced the challenge of time-synchronizing the different devices, which are by default not synchronized in time or frequency. For the frequency synchronization we used an external clock distributor. For the time synchronization we employed a new technique which employs the use of the long training sequence of the IEEE 802.11 protocol. We transmit the sequence, and an algorithm performs cross-correlation of the received signal on the array, with the known sequence. With this technique we are able to detect the sequence at each of the receiving streams and remove any phase offset between them. We showed that at a 9 dB SNR level the sequence is detected at 50% of the time, so with an efficient peak detection algorithm in place the sequence can be detected even in low SNR levels.

Finally, we presented a comparison between various antenna array geometries in the context of DoA estimation. We tested a square, a circular an L-shaped and a new, proposed by us antenna geometry, the articulated L-shaped array. We showed that in the majority of the cases the square and circular arrays have similar performance, while the articulated L-shaped array performs well in scenarios where the actual frequency of the signal is different from the frequency for which the element spacing of the array was calculated. The L-shaped array presented the lowest performance in most scenarios.

5.1 Future Work

Our system is described and evaluated through simulations in this study. Since the ground in the theoretical aspect has been laid, the next step is for METAL to be implemented as a functioning system using a software platform, possibly the GNU Radio SDR platform. A system operating in actual position estimation scenarios can face challenges not predicted during the theoretical modeling, and this will be an interesting case for further enrollment in the software implementation of METAL.

Adding to that, further work can be made in the area of the peak detection and outlier detection algorithms. In the first case, an efficient peak detection algorithm can significantly improve the accuracy of detection of the training sequence, helping not only the time-synchronization of multiple SDR devices but also the direct path detection in a multipath environment. In the second case, a smarter outlier detector can potentially reduce further the estimation error, especially in the case of smaller arrays, which could reduce the array size of the base stations and at the same time keep the error at low levels.

Concluding, the case of exploiting the DoA estimations of the reflected signal components for improving target detection should be investigated. The components that have an adequate amount of power to be detected by the MUSIC algorithm could be used, along with geometry manipulation, in order to find the junction point in the space, of the direct path and the reflected paths. That point will be the origin of the transmitter. This way not only the direct path component, but also the reflected ones will be exploited in the estimation process.

Bibliography

[1] L. Chen *et al.*, "Multiple emitter location and signal parameter estimation," *IEEE Trans. Antennas Propagat.*, vol. 34, pp. 276 – 280, 1986.

[2] R. R. and K. T., "Esprit estimation of signal parameters via rotational invariance techniques," *IEEE Trans. Acoust. Speech Signal Process.*, vol. 37, pp. 984 —- 995.

[3] Y. D. Huang and M. Barkat, in *Near-field multiple source localization by passive sensor array*, vol. 39, no. 7, 1991, pp. 968 – 975.

[4] L. J. X. Z. B. Ji *et al.*, "A computational efficient algorithm for joint range-doa-frequency estimation of near-field sources," *Digital Signal Processing*, vol. 19, no. 4, pp. 596 – 611, 2009.

[5] Y. W. G. Liao and H. C. So, "A fast algorithm for 2-d direction-of arrival estimation," *Signal Processing*, vol. 83, pp. 1827 – 1831, 2003.

[6] M. B. S. Marcos, A. Marsal, "The propagator method for source bearing estimation," 1995, pp. 121 — 138.

[7] M. R. A.-S. A. Pezeshki and M. Hohil., in *Wideband DOA estimation algorithms for multiple target detection and tracking using unattended acoustic sensors*, vol. 5417, 2004, pp. 1 – 11.

[8] Z. M. L. Z. T. Huang and Y. Y. Zhou, in *Direction-of-arrival estimation of wideband signals via covariance matrix sparse representation*, vol. 59, no. 9, 2011, pp. 4256 – 4270.

[9] R. Xiaowei *et al.*, "Estimation of 2-d doa using non-circular music method for uniform circular and rectangular arrays," *Journal of Electronics (China).*

[10] A. Y. J. Chan and J. Litva, "Music and maximum likelihood techniques on two-dimensional doa estimation with uniform circular array," vol. 142, no. 3, 1995, pp. 105 – 114.

[11] Z. Y. L. Xiang and X. Xu, "Doa estimation with circular array via spatial averaging algorithm," *IEEE Antennas Wireless Propag. Lett.*, vol. 6, p. 74–76, 2007.

[12] H. Sarkar *et al.*, "An l-shaped array for estimating 2-d directions of wave arrival," *IEEE Trans. Antennas Propagation*, vol. 39, no. 2, pp. 143 – 146, 1991.

[13] F. H. Changuel H. and A. Gharsallah, "2-l-shape two dimensional arrival angle estimation with a classical subspace algorithm," *Progress In Electromagnetics Research, PIER 66,*, pp. 301 – 315, 2006.

[14] P. M. G. and C. M. T., in *Azimuth and elevation angles estimation using 2-D MUSIC algorithm with an L-shape antenna.*, 2010.

[15] Y. Albagory and A. Ashour, "Music 2d-doa estimation using split vertical linear and circular arrays," *Int. J. of Computer Network and Information Security (IJCNIS)*, vol. 5, no. 8, p. 12, 2013.

[16] M. Ren and Y. X. Zou, "A novel multiple sparse source localization using triangular pyramid microphone array,," *IEEE Signal Processing Letters*, vol. 19, no. 2, pp. 83 – 86, 2012.

[17] Y. P. F. Yang and Z. Nie, in *DOA estimation with subarray divided technique and interporlated esprit algorithm on a cylindrical conformal array antenna*, vol. 103, 2010, pp. 201 – 216.

[18] S. Sen, J. Lee, K.-H. Kim, and P. Congdon, "Avoiding multipath to revive inbuilding wifi localization," in *Proceeding of the 11th annual international conference on Mobile systems, applications, and services.* ACM, 2013, pp. 249–262.

[19] S. Sen, B. Radunovic, R. R. Choudhury, and T. Minka, "You are facing the mona lisa: spot localization using phy layer information," in *Proceedings of the 10th international conference on Mobile systems, applications, and services.* ACM, 2012, pp. 183–196.

[20] M. Kotaru, K. Joshi, D. Bharadia, and S. Katti, "Spotfi: Decimeter level localization using wifi," in *ACM SIGCOMM Computer Communication Review*, vol. 45, no. 4. ACM, 2015, pp. 269–282.

[21] S. Gesbert *et al.*, "From theory to practice: An overview of mimo space–time coded wireless systems," *IEEE Journal on Selected Areas in Communications*, vol. 21, no. 3, 2003.

[22] S. M. Alamouti, "A simple transmit diversity technique for wireless communications," *IEEE Journal on selected areas in communications*, vol. 16, no. 8, pp. 1451–1458, 1998.

[23] Shannon's law. [Online]. Available: https://en.wikipedia.org/wiki/Shannon%E2%80%93Hartley_theorem

[24] C. Stoeckle, J. Munir, A. Mezghani, and J. A. Nossek, "Doa estimation performance and computational complexity of subspace-and compressed sensing-based methods," in *Smart Antennas (WSA 2015); Proceedings of the 19th International ITG Workshop on.* VDE, 2015, pp. 1–6.

[25] Armadillo: C++ Linear Algebra library. [Online]. Available: http://arma.sourceforge.net/

[26] openBLAS: An optimized BLAS library. [Online]. Available: http://www.openblas.net/

[27] LAPACK: Linear Algebra PACKage. [Online]. Available: http://www.netlib.org/lapack/

[28] International Telecommunications Union. [Online]. Available: http://www.itu.int/

[29] ITU recommendation. [Online]. Available: https://www.itu.int/dms_pubrec/itu-r/rec/m/R-REC-M.1225-0-199702-I!!PDF-E.pdf

[30] Ettus Research. [Online]. Available: http://home.ettus.com